FOREWORD

This report was prepared by the Missile and Space Vehicle Department of the General Electric Company, Philadelphia, Pa., on Air Force contract AF 33(616)-7579, under Task No. 314506 of Project 3145, "Investigation and Flight Test of Ion Exchange Membrane Fuel Cells." The work was administered under the direction of the Flight Accessories Laboratory, Aeronautical Systems Division. Capt. G. E. Starkey was project engineer for the Laboratory.

The studies presented extended from October, 1960 to November, 1961. Although the studies were a group effort, the chief contributors and their fields of interest were: B. Klawans, Project Manager; M.D. Read, Project Engineer; W. Haggerty, Flight Test; J. Bone, Battery Design; H. Zettick, Instrumentation; W. Losew, Laboratory Test; and B. Smith, Electrodes.

The cooperation of the Air Force which supplied and manned the KC-135 aircraft and made available "piggy back" RVX space for the zero g flight experiments is gratefully acknowledged.

In addition, MSVD is appreciative of the life cycle testing accomplished at ASD under the direction of Lt. M. Rutkowski.

ABSTRACT

This work was undertaken to determine the operating capabilities of General Electric Company's hydrogen-oxygen regenerative fuel cell which employs an anion membrane as a matrix to immobilize the potassium hydroxide electrolyte.

A series of life cycle tests was carried out in the laboratory with both single cells and multicell units. The results of single cell tests are quite satisfactory, however, multicell units as presently designed do not show comparable life.

A flight test on an aircraft was initiated to determine the effect of a limited time zero gravity environment on fuel cell operation. The environmental conditions imposed by these flights did not have an appreciable effect on fuel cell operation as determined by oscillograph recordings and photographs taken of the unit during the flights.

In an attempt to investigate fuel cell operation over a longer period of weightlessness, fuel cell modules were designed and built for flight testing as an experiment on an RVX. Unfortunately, the vehicle veered off course and had to be destroyed before conclusive data could be obtained.

PUBLICATION REVIEW

The publication of this report does not constitute approval by the Air Force of the findings or conclusions contained herewith. It is published only for the exchange and stimulation of ideas.

TABLE OF CONTENTS

LIST OF FIGURES

TABLES

1.0 INTRODUCTION

The hydrogen oxygen regenerative fuel cell battery is a promising new space power source because of its potentially high energy-per-pound level. Ground tests have proved the feasibility of this system in a gravity field, and have demonstrated adequate operational life times. However, little is known about the transport of the water vapor-liquid in a zero g field that is generated during the discharge cycle and consumed during the charge cycle of the batteries under consideration. One acid type thirty minute zero g flight in the RVX-2A nose cone re-entry vehicle gave no information. A second indicated constant operation at 20 percent of the design value from before take-off to impact perhaps because of a long shelf life history.

The Aeronautical Systems Division of the Air Force granted a contract in September 1960 to determine (by actual test of experimental regenerative fuel cell batteries under partially simulated orbital conditions) whether fuel cell state-of-the-art has advanced sufficiently for use as space vehicle energy storage devices.

A three phase program on anionic (basic) type fuel cells was initiated that included:

a) Laboratory tests of single and multicell units in various attitudes to develop operating and design information which would lead to a multicell unit capable of being cycled for thirty days of continuous operation in the space environment.

b) KC-135 flight tests of cycling single and multicell units to study operation in a limited duration zero g field under visual observation, human controllable, and highly instrumented conditions.

c) Extension of the KC-135 zero g time interval by a RVX piggyback 30-minute ballistic flight test of a multicell unit under limited instrumentation conditions.

Indicated design improvements were incorporated in components throughout the investigation.

Manuscript released by the author January 1962 for publication as an ASD Technical Documentary Report.

2.0 THEORY OF OPERATION

Regenerative, as the term is applied to the regenerative fuel cell battery, means that after the battery has discharged its stored energy, it is capable of being recharged. The completion of both the discharge and charge processes constitutes one complete cycle. Because the operation of all of the cells is the same, only one cell of the complete battery will be considered. It must be remembered, however, that the cells are connected in series in the battery and that the voltage of all cells is additive.

In a simplified fuel cell, the cavity (half-cell) on the left contains hydrogen gas (H_2), and the cavity on the right contains oxygen gas (O_2). When the fuel cell exists in this condition - both half-cells filled with their respective gases - the fuel cell is in the charged state.

When the cell is to be operated, or discharged, an external electrical load must be connected between the positive and negative terminals so a complete electrical circuit is formed. When the load is connected, a series of simultaneous electrochemical events occurs which causes electron flow through the external circuit.

2.1 Discharge

Briefly, what occurs during the discharge part of the regenerative cycle is as follows: In the hydrogen half-cell, hydrogen atoms absorbed on the catalyst combine with OH^- ions from the electrolyte to produce water and release two electrons. These electrons pass through the external circuit to the oxygen electrode. Here the oxygen on the surface of this electrode accepts the electrons and combine with water to form OH^- ions. The equation below illustrates the fuel cell reactions with a basic electrolyte.

$$H_2 + 2OH^- \rightarrow 2HOH + 2e \quad (H_2 \text{ electrode})$$

$$1/2\ O_2 + HOH + 2e \rightarrow 2OH^- \quad (O_2 \text{ electrode})$$

$$H_2 + 1/2\ O_2 \rightarrow HOH \quad \text{(overall fuel cell)}$$

2.2 Charge

During the charging part of the cycle, an external electrical source is connected to the cell, such that electrons will enter the fuel cell at the hydrogen electrode. This is the reverse of the discharge part of the cycle in which electrons left the hydrogen electrode. As a result of the reversed electron flow, the chemical reactions are opposite to those that occur during the discharge part of the cycle. This means that the electrons entering at the hydrogen electrode from the external source react with the water contained in the matrix to form hydroxyl ions and hydrogen atoms in the hydrogen

half-cell. The hydrogen atoms, which absorb on the platinum catalyst, leave the platinum catalyst and form hydrogen molecules (H_2) in the gaseous state. The hydroxyl ions thus formed travel through the matrix to the oxygen electrode, where they react to form oxygen (O_2) and give up electrons. Both gases, hydrogen and oxygen, are stored in their respective half-cells until the discharge part of the regenerative cycle again occurs.

2.3 Choice of Membrane

The acidic membranes used in the regenerative fuel cell efforts prior to this contract had extreme corrosion characteristics during the charge cycle. They also had very poor shelf life. Preliminary surveys indicated that the use of anion exchange membranes offered much less internal resistance when equilibrated with potassium hydroxide and showed promise of less corrosion and longer life capabilities. Accordingly, all commercially available anionic membranes were examined. The most promising, made by United Water Softeners Limited, Gunnersbury Avenue, London, England, was chosen for use on this program.

3.0 LABORATORY TESTS

3.1 Single Cell Cycling Tests

Single cell work was concerned with life cycling tests to develop information which would be of value in designing a satisfactory ten cell 50-watt fuel cell battery.

3.1.1 Cell Description

Electrodes - Platinum black was slurried with distilled water and a small amout of Teflon "30" emulsion (E.I. DuPont). Proportions varied depending on the various batches of platinum black used. The slurry was then spread on an aluninum foil and allowed to dry. Next the material was cured in a press, the temperature and pressure varying, again, with the particular batch of platinum used. The cured electrode was quenched in cold water and the aluninum dissolved from the electrode in a dilute caustic bath. Following thorough rinsing with distilled water, the resultant electrode which was a film about 1/2 mil thick and the desired diameter was air dried and stored until needed.

Electrolyte - The ion exchange membrane used was a Zerolit ion-exchange membrane, type A-20, hydroxide form, i.e. the mobile ion in the membrane is OH^-. This membrane is a proprietary product of United Water Softeners who will issue no further information concerning its composition or method of manufacture.

Mechanical description - An electrode was held in place against each side of the membrane by means of a #16 wire mesh screen. Stainless steel screening was used in the earlier models while nickel was used for the later units. The circular cell casings were fabricated from stainless steel stock and had gas spaces machined into them in the ratio of two volumes for hydrogen to one for oxygen. The screening was supported by means of ribs remaining in the housings. The entire assembly was held together by "C" clamps or bolts and sealed by means of "O" rings. A picture of a partially assembled test cell is shown in Figure I.

3.1.2 Test Procedures

The test procedure consisted of a 90-minute cycle, 55 minutes charge and 35 minutes discharge. The fuel cell was charged with external power to a terminal pressure of about 100 psig. At this point a pressure switch cut off charge current and held the cell on open circuit until the timer moved into the discharge phase of the cycle. The cell then discharged through a constant load for 35 minutes. Each cycling panel contained H_2 and O_2 gages, a pressure equalization chamber, and the required relays and valves. All panels worked from a common timer. In some instances a pressure transducer was used

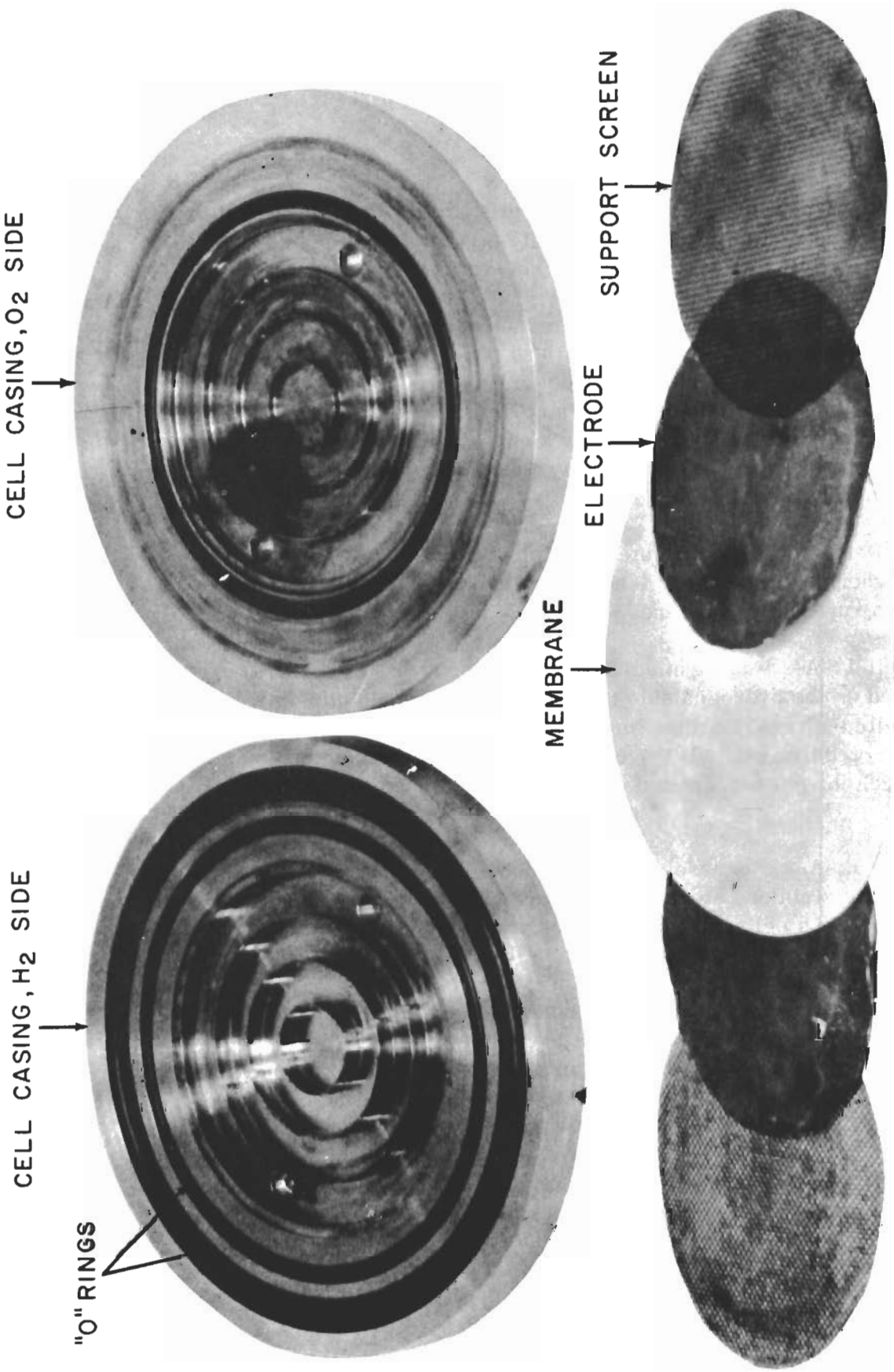

Figure 1. A Partially Assembled Fuel Cell

making it possible to obtain a print-out of cell pressure as well as cell voltage. Figure 2 shows the press used for curing electrodes and the cycling panel set-up.

3.1.3 Single Cell Test Results

Most of the single cell work was done with cells having electrodes of 12 in.^{2} area (about 4-inches diameter). One cell of 64 in.^{2} area (9-in. diameter electrodes) was cycled. Test results are noted in Table I.

12-A-3 - Cell 12-A-3 had stainless steel screens and housing. It operated for 993 cycles until an external power failure caused the cell to go into an extended discharge from which the cell could not recover. The electrochemical efficiency (amp-minutes out)/(amp-minutes in) was 80 to 100 percent. The energy efficiency (watt-minutes out)/(watt-minutes in) remained at about 33 percent for the duration of the test. Detailed data on cell 12-A-3 are presented in Table II.

12-A-4 - Cell 12-A-4 was originated to duplicate 12-A-3. The test was terminated when an external gas leak caused unequal internal pressures resulting in a ruptured membrane.

12-A-7 - Cell 12-A-7 was identical to 12-A-3 except that filter paper was employed on the hydrogen side to keep the membrane uniformly moist. It failed after 434 cycles for the same reason 12-A-3 failed. It should be noted that cell 12-A-7 operated at an electrochemical efficiency of 90 to 100 percent and an energy efficiency of about 43 percent.

12-A-8 - No. 12-A-8 was assembled with nickel screens in place of stainless steel. The stainless steel cell casings were used, however. Nickel was substituted for the steel screens when it became evident that the stainless was corroding and causing degradation in cell performance. The data for 12-A-8 is tabulated in Table II. From this we note that 12-A-8 performed at a relatively high energy efficiency, about 50 percent, and an electrochemical efficiency of over 95 percent. This unit cycled until an external fitting failed, releasing the stored gases. Figure 3 is a typical initial polarization curve for a cell using nickel screen construction, depicting both the charge and discharge phases of fuel cell operation.

12-A-10 - The primary puspose of cell 12-A-10 was to determine operating characteristics of the fuel cell at higher current densities. The unit was charged to 120 psig and operated through a 90-minute cycle. It was initially charged at a rate of 2.95 amps (38 ma/cm^2) and discharged at a 4 amperes (49 ma/cm^2).

TABLE I

CYCLING TESTS WITH SINGLE CELLS

Unit	Electrode Area ($in.^2$)	Start Date	Finish Date	Duration of Cycling (days)	No. of Cycles	Charge ($ma./cm.^2$)	Discharge ($ma./cm.^2$)	Electrochemical Efficiency (%)	Energy Efficiency (%)
12-A-3	12	9/13/60	11/18/60	64	993	12	16	81 - 90	31 - 36
12-A-4	12	9/9/60	10/4/60	25	333	12	16	95 - 100	38 - 42
12-A-7	12	10/20/60	11/17/60	28	434	12	16	87 - 90	43 - 46
12-A-8	12	1/19/61	2/1/61	13	175	12	16	96 - 100	49 - 54
12-A-10	12	3/20/61	4/26/61	37	584	36	38	89 - 93	27 - 30
64-A-5	64	12/5/60	2/13/61	70	1067	11	14	91 - 97	16 - 45

TABLE II

A. DATA FOR CELL 12-A-3 (STEEL SCREENS)

Cycle	Charge				Discharge				Electro-chemical Efficiency (%)	Energy Efficiency (%)
	Current (amp.)	Voltage (volts)	Time (min.)	Amp. - min.	Watt - min.	Current (amp.)	Voltage (volts)	Time (min.)	Amp. - min.	Watt - min.	
100	0.88	1.65	55	48	80	1.30	0.69	30	39	27	81	34
303	0.88	1.65	55	48	80	1.20	0.62	39	47	29	98	36
502	1.10	1.70	45	50	84	1.28	0.64	35	45	29	90	34
725	1.10	1.73	48	53	91	1.30	0.66	35	46	30	87	33
886	1.10	1.80	45	50	89	1.24	0.64	35	43	28	86	31
993	1.10	1.75	45	50	86	1.24	0.64	35	43	28	86	33

B. DATA FOR CELL 12-A-8 (NICKEL SCREENS)

20	1.20	1.59	39	47	74	1.26	0.85	37	47	40	100	54
99	1.20	1.56	35	42	66	1.20	0.82	34	41	33	98	50
175	1.20	1.62	37	44	72	1.20	0.84	35	42	35	96	49

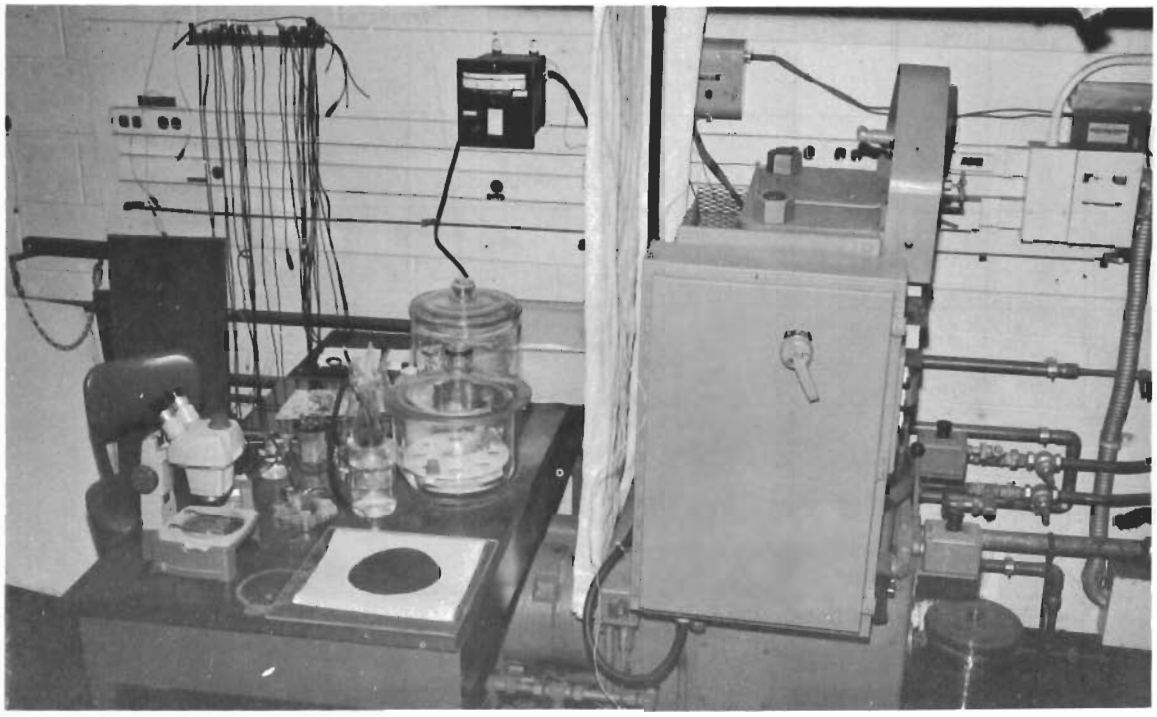

a. Electrode Press

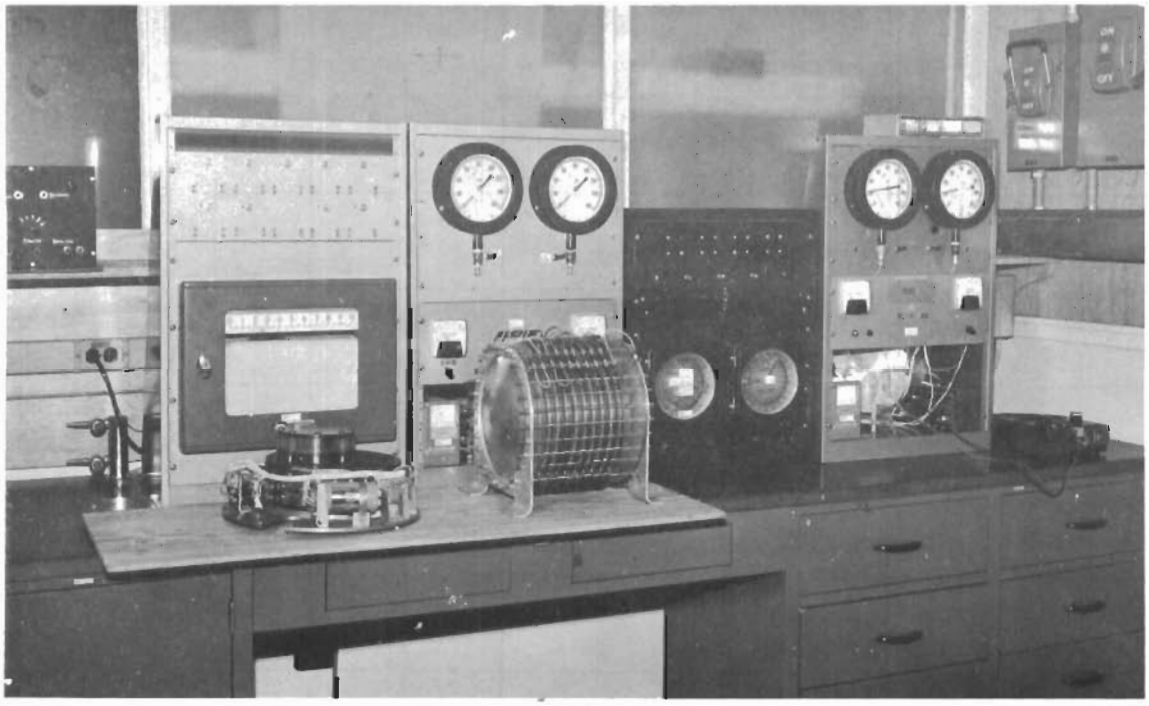

b. Cycling Panel Set-up

Figure 2. Fuel Cell Facilities

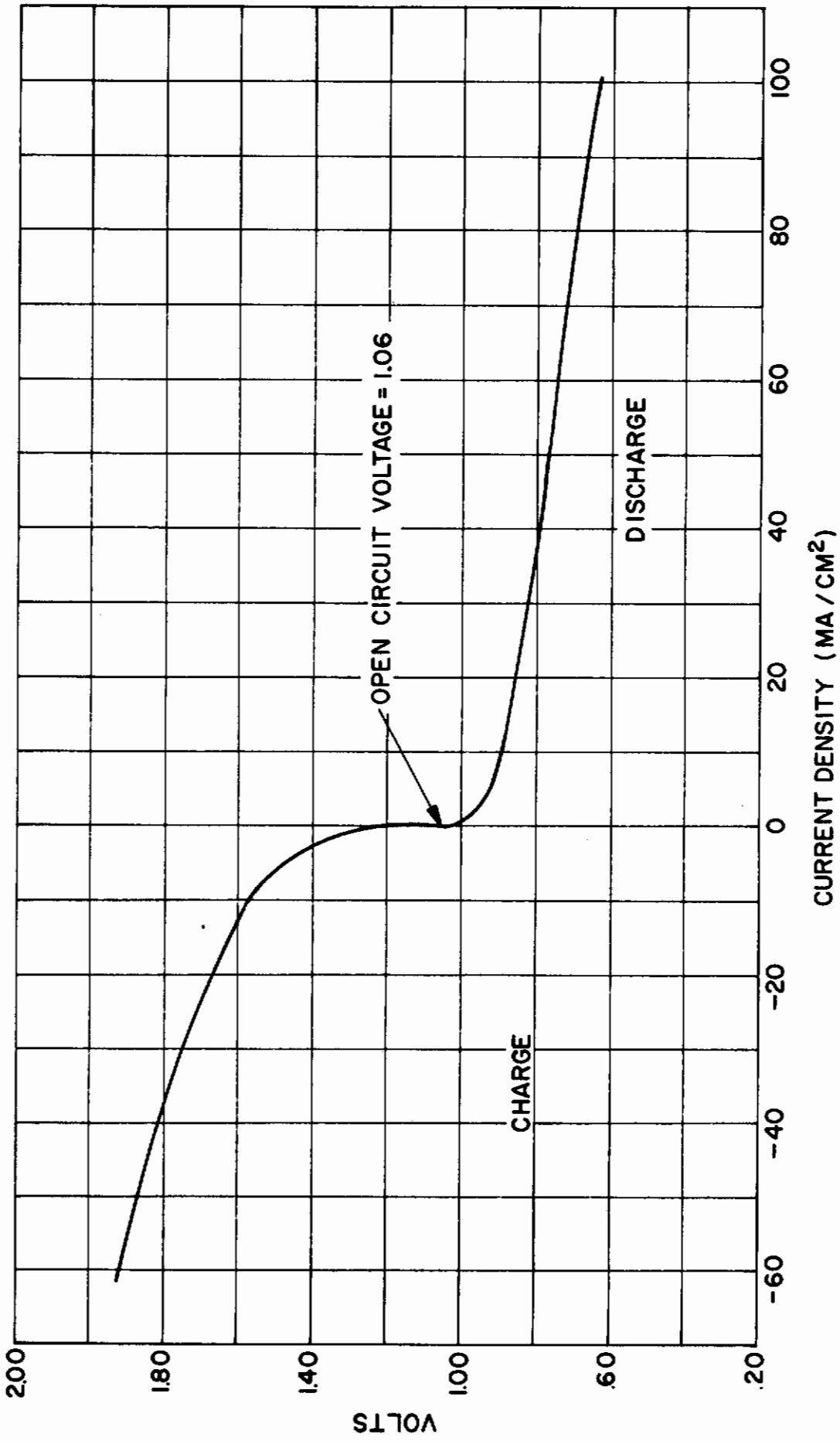

Figure 3. Typical Initial Polarization Curve for Single Cell with Nickel Screens

This cell was also operated in horizontal and vertical positions. It was observed after a few cycles that the cell was position sensitive, indicating water removal was a problem at higher current densities. On this basis the cell was rebuilt using wicks. The performance improved considerably in that the unit did no show as great a positon sensitivity as it did before wicks were installed. However, performance did tend to drop off with cycling, indicating that the wicking system needed more development. After 217 cycles discharge current had dropped to 2.20 amps (27 ma/cm^2) and energy efficiency from 47 percent to 33 percent. This unit failed on burnout after 584 cycles.

64-A-5 - Cell 64-A-5 was assembled using 9-inch diameter electrodes and stainless steel screens and housings. It operated through 1067 cycles and was disassembled for observation before failure occurred. Performance had dropped off considerably during cycling, from an original 47 percent energy efficiency to about 17.5 percent efficiency. This degradation could be due to several things: (a) contamination from stainless steel, (b) pin hole leak in the membrane or (c) drying out of the upper part of the membrane due to the membranes poor wicking ability. When disassembled, considerable corrosion of the screens and housing was noted and the electrodes were found to be fragmented. The latter was due to the constant pressure of the screens and also probably to oxidation of the electrode on the oxygen side.

3.2 Multicell Cycling Tests

Multicell units were fabricated and tested to establish the cycle capability of the regenerative fuel cell battery. An assembly drawing of the ten cell 50-watt flight unit is shown in Figure 4.

3.2.1 Multicell Unit Description

Six 64-square inch electrode area multicell batteries have been built. The principle of assembly for the multicell units is the same as for single cells, however, the method of internal support is quite different. Multicell units use a system of screens supported by neoprene sponges, the screens being attached to bipolar current collectors by small metal tabs. The current collectors extend beyond the cell wall and so act as thermal paths for the removal of heat from the membranes. Cell walls are of Lucite and end caps are of steel. Each multicell unit contains a pressure equalization chamber consisting of a hydrogen and oxygen chamber separated by a flexible rubber diaphragm. All oxygen chambers of each cell are manifolded together with the pressure equalization chamber as are the hydrogen chambers. A picture of a ten cell 50 watt unit is shown in Figure 5. The ten cell unit weighs about 44 pounds. A component weight breakdown is given in Table III.

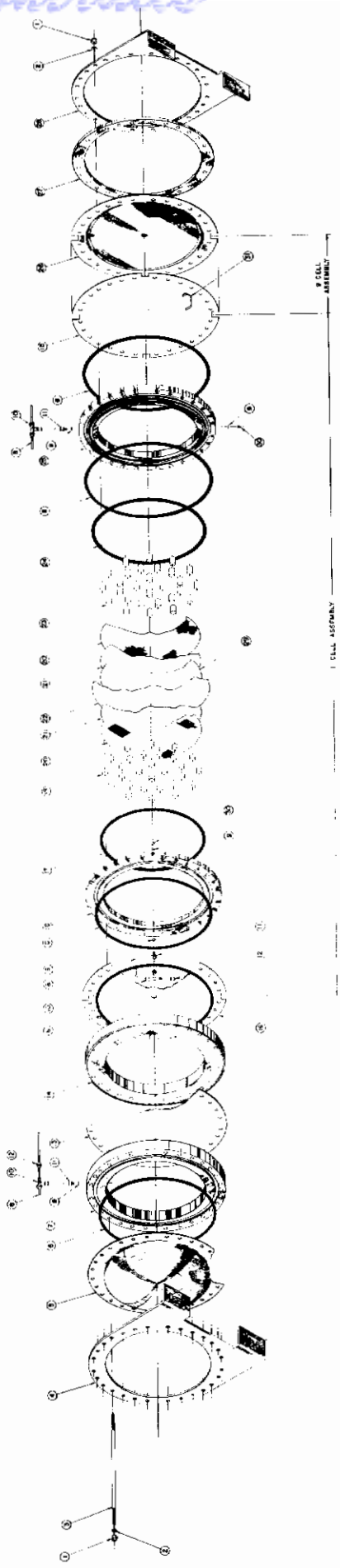

Figure 4. Assembly Drawing of the Ten Cell 50-Watt KC-135 Flight Unit

LEGEND

INDEX NUMBER	ITEM	DRAWING NUMBER
1	NUT, HEX SELF LOCKING	
2	WASHER	
3	STUD WITH INSULATING SLEEVE	SK56102-599-10P1
4	MOUNTING BRACKET	SK56102-599-14P1
5	END CAP ASSEMBLY	SK56102-599-9G2
6	O-RING	
7	RING, H_2 (BELLOWS)	SK56102-599-13P1
8	MANIFOLD TUBING	
9	O-RING	
10	FITTING, TEE	
11	FITTING	SK56102-599-6P1
12	FITTING	
13	DIAPHRAGM	SK56102-599-15P1
14	RING, O_2 (BELLOWS)	SK56102-599-12P1
15	CELL WALL	SK56102-599-5P1
16	CELL WALL	SK56102-599-5P2
17	O-RING	
18	RING, O_2	SK56102-599-7P1
19	SPACER (OXYGEN)	
20	SCREEN	SK56102-599-4P1
21	WAFER	SK56102-599-3P1
22	MEMBRANE	SK56102-599-2P1
23	SPACER (HYDROGEN)	
24	O-RING	
25	RING, H_2	SK56102-599-8P1
26	END CAP ASSEMBLY	SK56102-599-9G1
27	INSULATOR	SK56102-599-11P1
28	MOUNTING BRACKET	SK56102-599-14P2
29	FILTER PAPER	
30	SCREW	
31	STAINLESS STEEL STRIP, BUS	

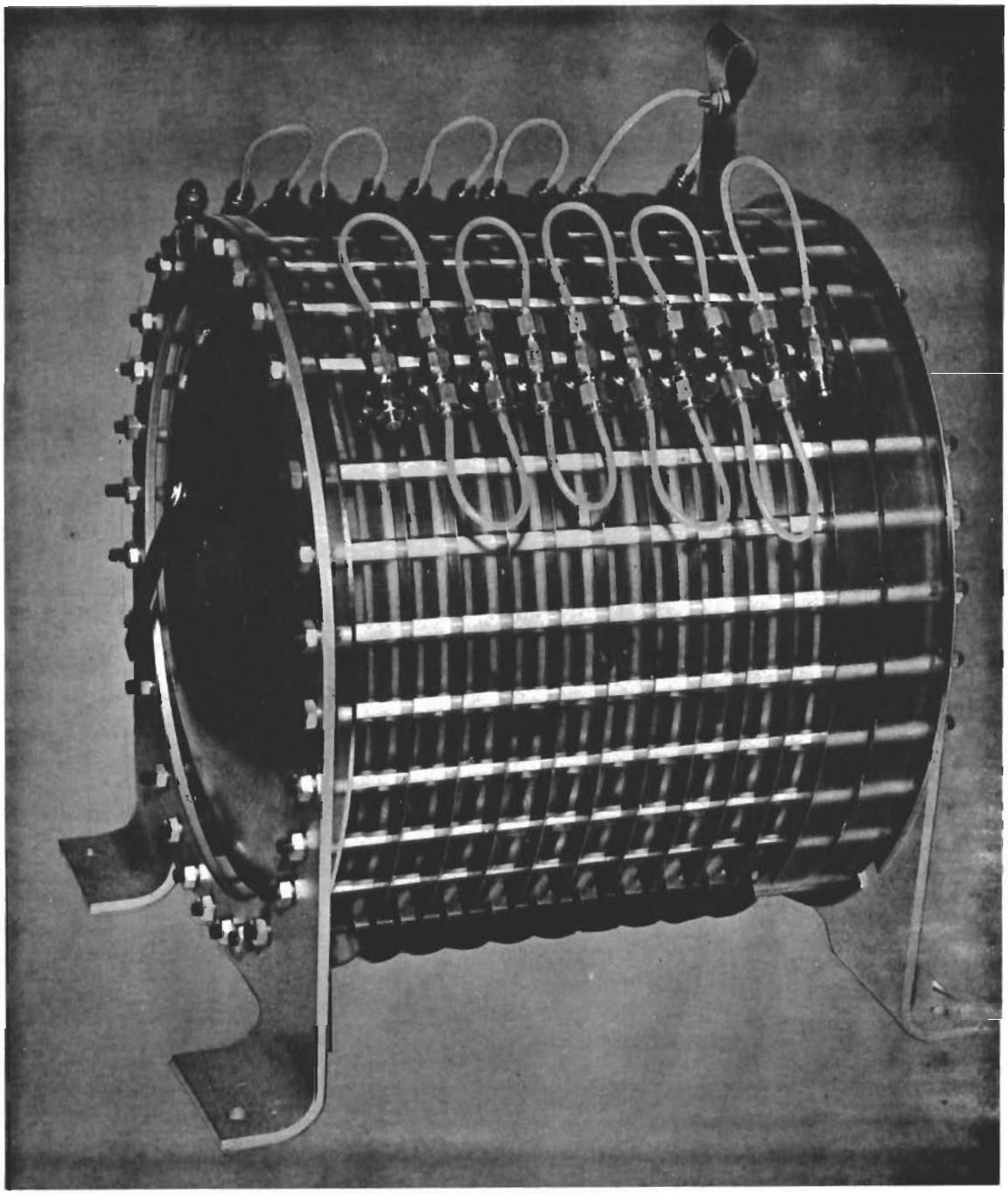

Figure 5. 50-Watt Regenerative Fuel Cell

Table III Component Weights of the 50-Watt Fuel Cell

Part Name	No. Per Battery	Wt. Each	Total Weight
Ring O_2 + "O" rings	10	230.2gm	2302 gms
Ring H_2 + "O" rings	10	336.2	3362
Cell Wall	10	155.0	1550
End Cap Bellows	1	1201	1201
End Cap H_2 Cell	1	1307	1307
Ring, Bellows	2	860	1720
Diaphragm	1	206.5	206
Mounting Bracket	2	554	1108
Insulator Ring	1	156	156
Fitting, Manifold	21	17.1	358
Fitting, Swagelock Tee	21	39.3	820
Tubing, Nylon	15 ft.	2.0	30
Studs with Insulation	28	71.5	2000
Neoprene Spacers, .875"	29	1.4	41
.625" (29)	261	1.3	339
.312" (29)	290	.7	203
Support Rings 8" x .645"	1	51.7	52
6" "	1	41.5	42
4"	1	24.4	24
2"	1	11.9	12
8" x .210	10	17.5	175
6" "	10	13.7	137
4" "	10	8.0	80
2" "	10	3.5	35
8" x .460	10	37.7	377
6" "	10	29.0	290
4" "	10	17.3	173
2" "	10	8.25	83
Nuts 1/4" x 28	56	2.8	157
Washer 1/4"	56	.055	30
Plug Swagelock	4	8.1	32
Screws, Vent + "O" Ring	23	0.9gm	21
Screen, 15 x 15 mesh	20	36.0	720
Membrane	10	46.3	463
Wick (41-H Whatman)	10	22.0	220
Electrodes	20	10.50	210
Contacts, 1/4" x .002"	240	.13	31
		Total	20067 gm
			44 1/2 lb.

3.2.2 Multicell Test Results

The batteries were cycled through 90-minute cycles similarly to the single cell units. Current densities employed were of the same order as those used for most of the single cell work, 12 ma/cm^2 on discharge. A tabulation of multicell cycle tests is given in Table IV.

3.2.2.1 Unit 50-W-1

This unit was built with General Electric Company funds and tested under the present contract.

In the regenerative fuel cell it is necessary to remove all atmospheric oxygen from the hydrogen side of the fuel cell and the bellows expansion chamber. Failure to do so, particularly in the multicell units will result in a rapid combination of the atmospheric oxygen with the hydrogen formed during charge. This may very well cause a fire at the electrode surface which, of course, ruins the fuel cell. To eliminate this possibility all hydrogen chambers were purged with nitrogen gas. Unfortunately burnouts continued in the end-cells where air would be trapped in the dished end plates. This problem was solved by installing vent ports in the domed ends allowing complete purging. By the time the purging problem was solved, Unit 50-W-1 was "shop worn" by repeated assembly and disassembly because of burnouts from incomplete purging and would not seal properly for cycling purposes.

After effecting a satisfactory purge procedure a polarization run was made with unit 50-W-1. The maximum value obtained was 5.2 volts at 8 amps or 42 watts. Considering the shop worn condition of the unit at this point the 42-watt value was encouraging and indicated that 50 watts should be readily obtainable with a new unit.

25-W-1 - Unit 25-W-1 consisted of five cells salvaged from 50-W-1 and this unit operated for 128 cycles. Performance slowly deteriorated throughout the life of the unit culminating in a burnout of one of the end cells. From this it was deduced that the end cells needed reinforcing. This improvement was incorporated in all subsequent units.

3.2.2.2 Unit 50-W-3

Unit 50-W-3 was built incorporating certain modifications derived from an analysis of the operations of Unit 1. These included concentric plastic support rings for the membranes, reinforced cooling fins on the end cells, and complete testing of all membranes for pin holes before assembly. Initial polarization

TABLE IV

CYCLING TESTS WITH MULTICELL UNITS

Run No.	Time (min: sec)	Battery Voltage (Volts)	Current (Amps)	Single Cell Voltage (Volts)	O_2 Batt. Pressure (psia)	H_2 S.C. Pressure (psia)	Temperatures (^{o}F.) H_2 Batt.	H_2 S.C.	Batt. Fin	S.C. Fin	Ambient	Battery Condition
1	2:00	7.5	-5.6	.55	50	32.8	95.4	89.1	82.4	78.2	76.9	Discharge
2	7:20	20	7.1	2.00	52	33.3	93.9	88.1	82.4	77.0	74.7	Charge
3	14:40	20	7.1	2.00	61	35.4	84.1	88.7	82.6	77.0	73.3	Charge
4	20:00	20.4	6.4	2.03	69	38.0	94.8	89.2	84.0	75.3	72.4	Charge
5	23:50	20.4	6.4	2.03	73	40.2	95.0	89.8	85.0	74.0	71.8	Charge
6	28:50	7.5	-5.6	.52	71	40.4	97.8	91.2	83.0	73.5	71.0	Discharge
7	31:10	7.5	-5.6	.52	69	39.7	99.1	91.8	82.2	73.2	70.4	Discharge
8	36:00	7.5	-5.6	.52	61	37.4	101.9	93.0	83.1	73.0	69.7	Discharge
9	46:25	19.2	7.8	1.90	53	33.1	107.7	95.0	84.7	73.0	67.8	Charge
10	49:30	19.9	7.0	2.00	56	34.5	108.1	94.8	83.4	72.7	67.3	Charge
11	52:20	19.9	7.0	2.00	60	36.00	108.6	94.6	82.1	71.8	67.0	Charge
12	55:30	20.2	7.0	2.02	65	37.6	109.1	94.2	82.1	71.0	66.7	Charge
13	60:00	20.1	7.0	2.02	72	39.4	110.0	94.0	82.5	70.0	65.9	Charge
14	63:10	—	0	1.00	74	40.3	111.0	94.0	82.8	71.1	65.3	O.C.
15	66:00	7.5	-7.5	.48	73	40.4	112.4	94.0	83.0	71.8	65.0	Discharge
16	74:50	7.5	-7.5	.47	61	36.3	117.3	98.0	82.3	68.1	61.0	Discharge
17	78:00	6.9	-7.9	.40	55	33.7	120.1	100.5	82.1	68.9	61.0	Discharge
18	80:00	6.9	-8.0	.40	50	31.7	121.9	102.0	82.0	69.1	61.0	Discharge

for this unit was better than any obtained with a multicell unit up to that time. A polarization and power curve is shown in Figure 6. This unit operated uniformly at a charge rate of five amperes and a discharge rate of six amperes for 30 cycles. Following cycle 31, the charge voltage tapered off, cell #5 went into reverse, and at cycle #36 cell #5 burned out.

On occassion a cell may go into reverse during discharge of a multicell battery. This is caused by poor electrodes not sufficiently active to sustain operation at a positive voltage. When the poor cell is being driven by other more active cells polarization may be so great that the cell may actually reverse polarity. When this happens a tremendous amount of heat is released at the electrodes since the cell behaves as a resistive load. In extreme cases, where the negative voltage is high enough to overcome electrode over-voltages, hydrogen gas may be generated at the oxygen electrode and vice versa.

3.2.2.3 Unit 50-W-4

Unit 50-W-4 was the first unit assembled for the KC-135 test. Its poor performance may be largely attributed to external gas leaks.

3.2.2.4 Design Modifications

Unit 50-W-4A was built incorporating all improvements suggested to date. All new elements were fabricated with the exception of the domed end caps and legs. The improvements included:

a) Substitution of nickel screen and cell walls for the stainless steel used on all previous units. The steel was a major source of corrosion and electrode contamination where used. Nickel has shown no evidence of objectionable corrosion at this writing.

b) Improved membrane support for the end cells through reinforced end cell current collectors.

c) Decreased tolerances on manufactured parts to eliminate the external gas leakage problem.

Unit 50-W-4A was flown on the KC-135 through several limited time zero gravity maneuvers. During a flight in May of 1961, the unit was cycled seven times. It was reactivated in October and cycled for an additional nine cycles before failure. Upon disassembly it was observed that most of the membranes had failed by rupturing at the top. This indicates that the membranes had become dehydrated as a result of the five months stand between tests and the poor wicking qualities of this membrane prevented a uniform rewetting when cycling was resumed. As the membrane dried it tended to shrink, finally resulting in a rupture near the external "O" ring seal.

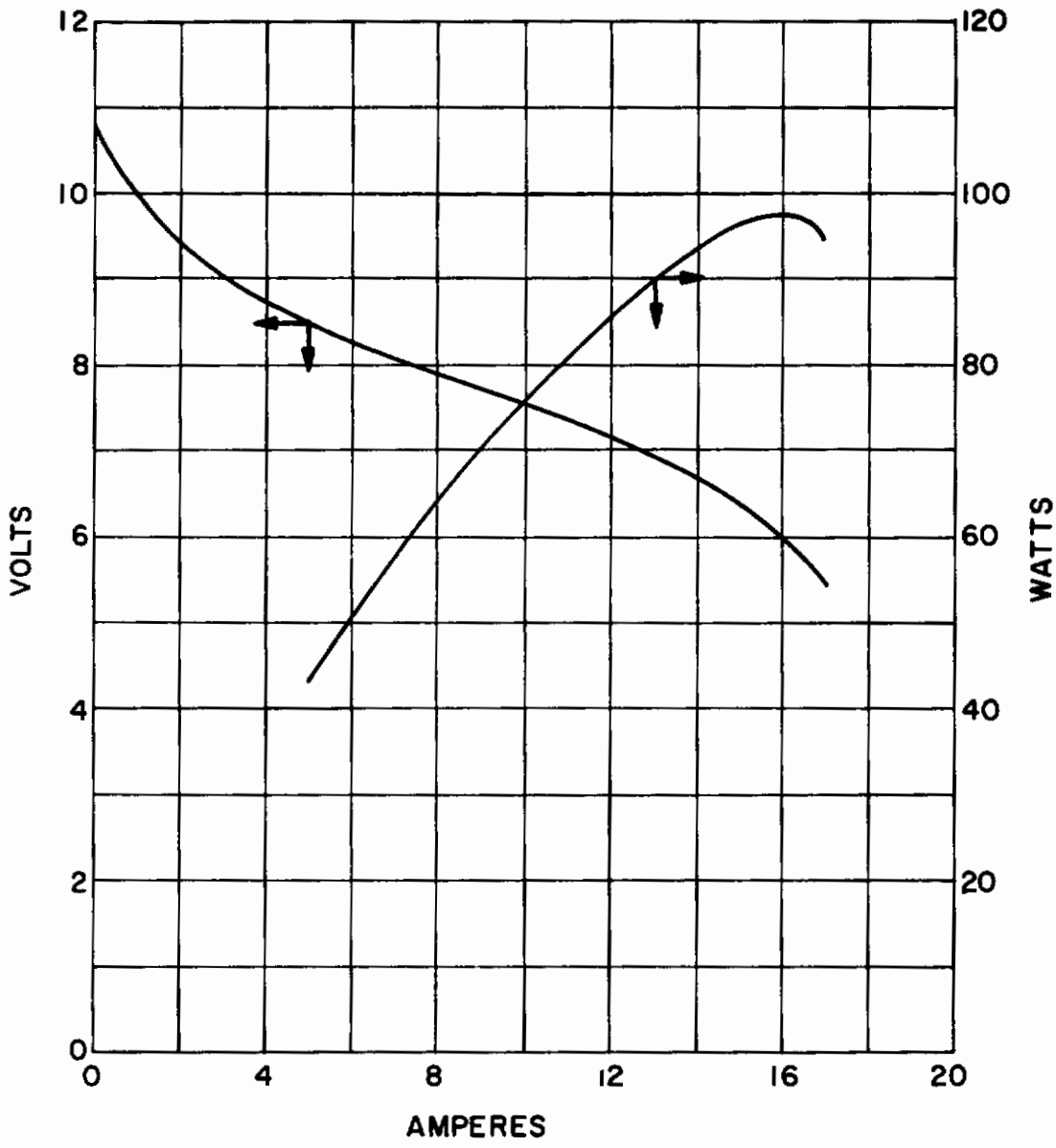

Figure 6. Polarization and Power Curve for 10 Cell Unit 50-W-3

Six cell unit - 50-W-4A was rebuilt into a six cell unit with new membranes and recoverable electrodes from the old unit. This battery was operated for 19 cycles before failure occurred. Operation was at a reduced level, two amperes and a average of 0.70 volt per cell, as compared with an expected 0.90 to 0.95 volts for new cells at two amperes. Upon disassembly of the six cell unit, portions of the nickel screen were observed to be covered with a green coating. This is believed due to oxidation of the nickel, a condition which is theoretically possible at the voltages used for charging the fuel cell. The nickel probably posesses sufficient passivity to prevent this from happening initially since in most cases the corrosion has not been observed on disassembled units containing nickel. However, it is possible that the surface of the screen changes sufficiently with usage to permit formation of the nickel oxide observed.

4.0 ZERO GRAVITY AIRCRAFT FLIGHT

4.1 Test Package Description

This test was designed to determine the operating characteristics of the regenerative fuel cell under a limited time zero gravity environment. Units to be tested included one ten cell 50-watt battery of conventional design and one single cell of 64 in.^{2} area assembled in a housing with clean lucite faces. The entire assembly was mounted on an aluminum test bed and flown on a KC-135 aircraft specially outfitted for zero gravity testing. A photograph of the test bed is shown in Figure 7.

The operation of the fuel cells was controlled from a panel located amidships in the aircraft. At this location, individual cell voltages were visually monitored and the units were cycled. Camera operation was also controlled here. Two direct read-out oscillographs were installed in the aircraft to record operating parameters.

4.2 KC-135 Flight Measurements

Instrumentation for the KC-135 flight tests included cameras, and pressure, temperature, g level, voltage and amperage measurements.

Cameras - Both still and motion pictures were obtained. The still photos were magnified to get a detailed view of the hydrolysis process. Motion pictures illustrated the overall process.

Instrumentation recorder - All measurements other than photographic were made on a Midwestern recorder having a high frequency (500 cps) response. Low lag transducers were used throughout. Wherever possible, inflight calibration check points were included in the permanent record.

Pressures - A differential pressure gage ($\pm$ 1 psi) was used to define the operation of the pressure equalization valve in the battery system. Aneroid cells (0-160 psi) gave the hydrogen and oxygen pressure levels.

Temperatures - Low lag temperature measurements at the surface of the cell membrane, at the middle and outer edge of the cooling fin, and outside the cell case (ambient) were made.

g levels - All three components of acceleration were measured. Lateral, directional and normal accelerometers had a range of 0-4 g. In addition, a normal accelerometer of $\pm$ 1 g range was used to closely define minor contacts.

Battery performance - Voltmeters (0-20 v) and ammeters (0-40 amps) were used to define battery performance in conjunction with the aneroid pressure measurements.

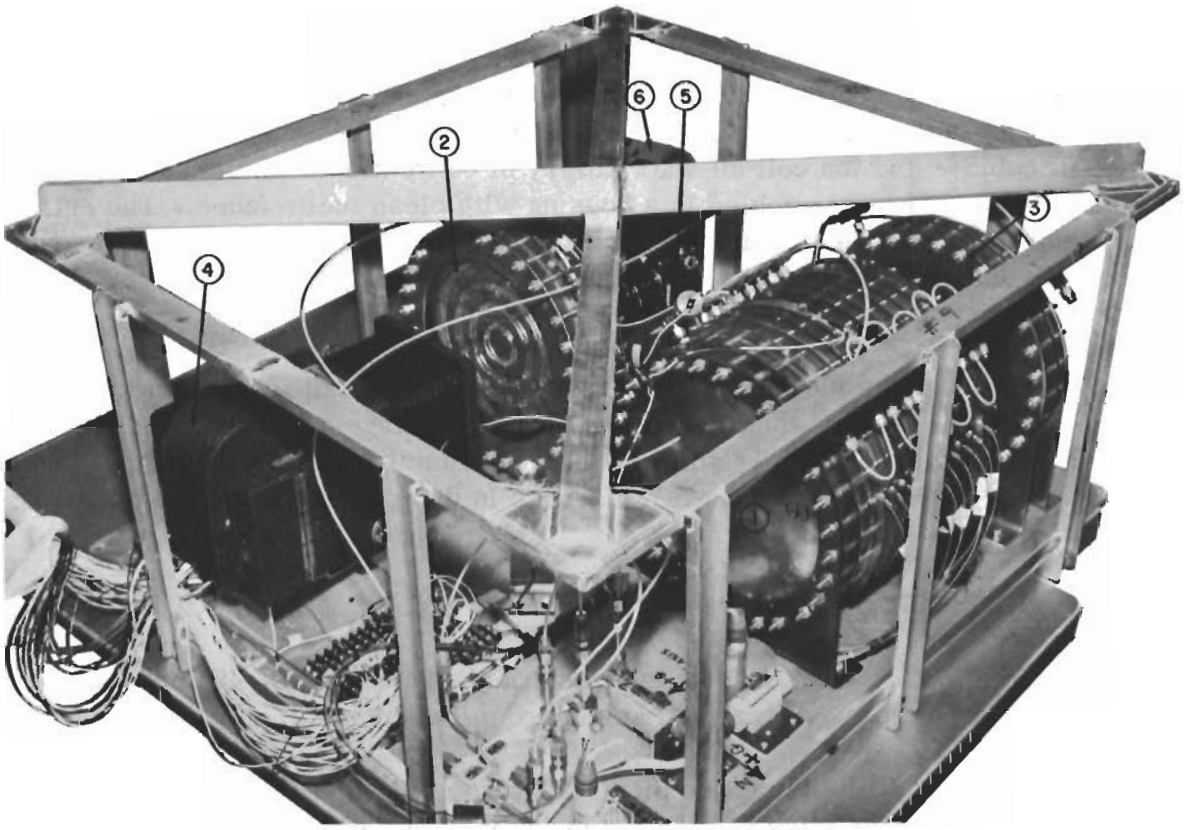

Figure 7. The KC-135 Fuel Cell Test Bed

1. 10 Cell 50-Watt Fuel Cell Battery
2. Single Cell with Lucite Walls
3. Pressure Compensating Chamber for Single Cell
4. 70 mm Sequence Camera
5. 35 mm Sequence Camera
6. High Speed Motion Picture Camera
7. Accelerometers
8. Pressure Transducers

4.3 KC-135 Zero Gravity Maneuver[1]

The airplane is trimmed in level flight, power MRT, at an altitude 500 feet below the point where $M_i = 0.865$ equals V_e Max (about 23,500 feet, depending upon the temperature). Power is increased to MRT until airspeed reaches V_e Max, and the aircraft climbs 500 feet with constant airspeed $M_i = 0.865$. Acceleration is increased smoothly to 2.5 "g" and held until reaching a 45^o pitch angle. The pilot pitches the aircraft forward approximately 10^o to achieve zero gravity. At this time, the co-pilot reduces power to maintain thrust equal to drag. The co-pilot, using the longitudinal accelerometer reference, continues to reduce power as the airplane ascends and increases power during descent. Recovery is initiated at a 45^o exit angle with idle power, a maximum normal acceleration of 2.5 "g" and a maximum airspeed of $V_e = 350$ knots. Stabilizer trim is not used for this maneuver because of the low service life of the stabilizer trim actuator clutches. The aircraft center of gravity is kept at 30.0% M. A. C. to reduce stick forces and to decrease the possibility of stick force lightening when maneuvering. (Figure 8)

4.4 Aircraft Flight Test

Data were recorded during 25 zero gravity maneuvers, seven during the first day's flight and eighteen during the second. An earlier flight was aborted due to an aircraft malfunction before any zero gravity maneuvers had been performed.

The ten cell battery and single cell were operated in series at currents of five to eight amperes. Even though the ten cell unit had been tested at rates up to 12 amperes (27 amperes/ft^2) for a few minutes in the laboratory, it was not possible to achieve this level in the aircraft. The primary reason was that all resistance pots on the test panel were shorted out in the laboratory, a procedure not considered safe in the aircraft. Secondly, a ten-foot cable was used in the laboratory compared to 50 feet in the aircraft.

Before the start of each flight the units were charged to full pressure - 60 psig for the battery and 25 psig for the single cell.

First flight The first flight consisted of seven zero gravity maneuvers with periods of weightlessness ranging between 10 and 20 seconds. During the flight the battery was cycled between 40 and 60 psig battery pressure for two cycles at a five-amp rate. Some difficulty was encountered with the flood lamps installed on the test shelf. The filaments could not stand the shock of pull-out and after three runs no lamps were functioning. However, the fuel cell did not appear to be affected by any portion of the maneuver.

Improved flood lamps were installed on the test shelf for the second flight. These lamps operated on 28 volts rather than the 110 volt lamps operated on in the first flight.

[1]See Energy Conversion for Space Power, Edited by N.W. Snyder Program in Astronautics and Rocketry Vol. 3 p 597.

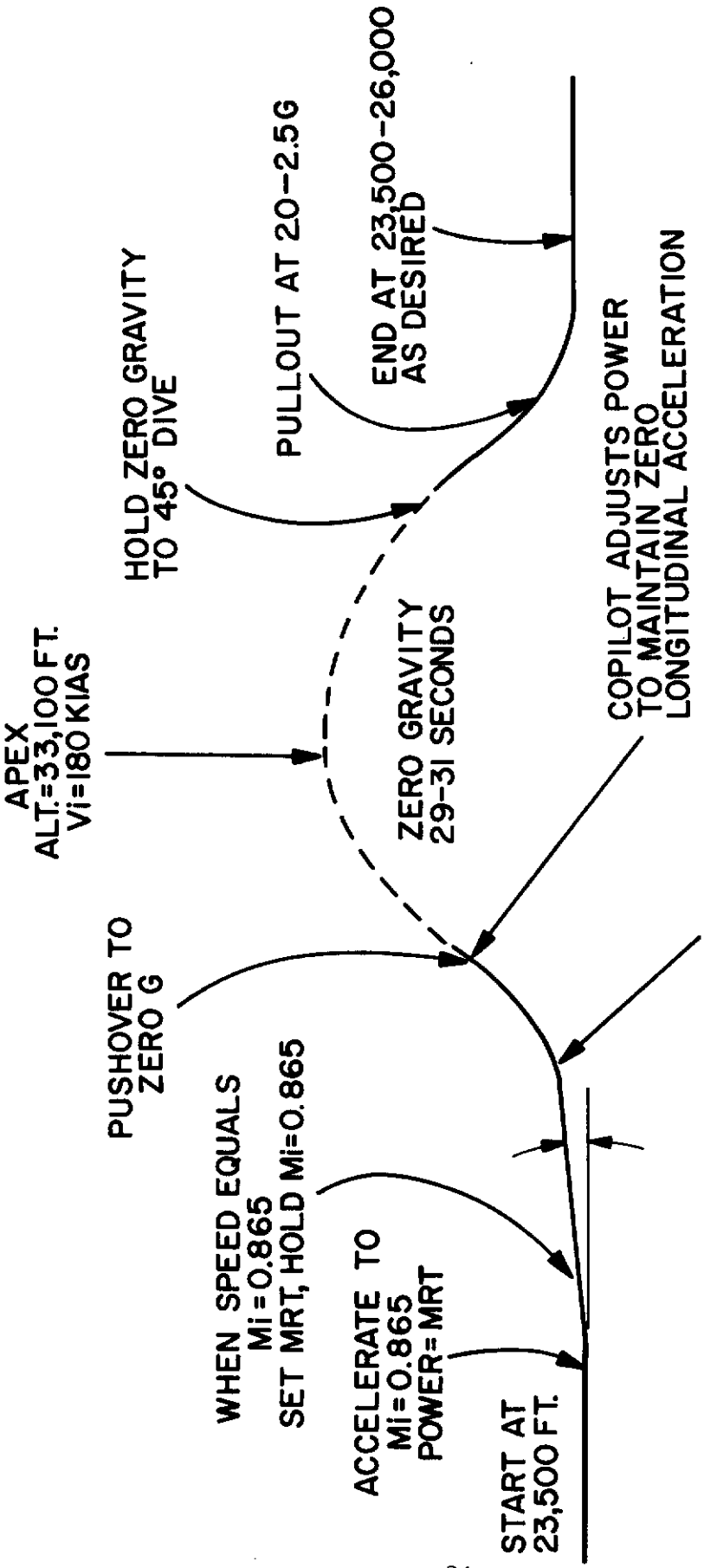

Figure 8. **Keplerian** Trajectory - KC-135 Airplane

Second flight Eighteen zero gravity runs were made. The fuel cells were put through two complete charge-discharge cycles while the current was varied between five and eight amperes. All instrumentation, lamps, and cameras worked satisfactorily. The control panel instrumentation indicated that the fuel cell was functioning properly at all times, a fact verified by the oscillograph records and the photographs of the single cell.

4.5 Data Presentation

First flight The data for the first days flight are summarized in Table V. Time is expressed in minutes and is referenced to the state of the first manuever. All readings presented were made during zero gravity.

Second flight Data from the second day's flight was selected for more comprehensive study since the flight covered a wider variety of operating conditions and these data could be correlated with that from the first flight. The start of the pull-up at initiation of the zero gravity maneuver is taken as zero time for each run. Data within a run are consistent with $\pm$ 0.5 second, while the relation of one run to another for a given flight has an accuracy of $\pm$ 30 seconds. Records of the complete second flight showing battery and single cell operating parameters are given in Table VI and Figures 9, 10 and 11.

Figure 12 represents a typical portion of one discharge cycle given in Figures 9, 10 and 11 on a greatly expanded time scale. Here it is possible to note the lack of any effect of g loading on fuel cell operation during a typical zero g maneuver.

4.6 Observations form Oscillograph Records

4.6.1 Camera Operation

Camera operating times are given in Table VII. During the first flight, the cameras were operated throughout portions of the complete maneuver. However, on the second flight, they were operated only during the zero gravity period for the first 14 maneuvers. Operation was then extended through pull-up for the next three, and for the complete maneuver on the last run. The camera operating times for the first fourteen runs agree very closely with the time at zero gravity.

4.6.2 Time of Runs

The time at zero gravity during the first flight varied widely with an average of about fourteen seconds. The second flight was made in smoother air and was more consistent with an average time at zero gravity of fifteen seconds. The time at zero gravity includes some perturbations, but the shock levels experienced from contact with the aircraft prior to pull-up were generally less than 0.5 g's **(see Figure 12).**

TABLE V

FUEL CELL OPERATING PARAMETERS DURING ZERO G

FLIGHT #1

Run No.	Time (min: sec)	Battery Voltage (Volts)	Current (Amps)	Single Cell Voltage (Volts)	O_2 Batt. Pressure (psia)	H_2 S.C. Pressure (psia)	Temperatures ($^oF.$) H_2 Batt.	H_2 S.C.	Batt. Fin	S.C. Fin	Ambient	Battery Condition
1	00:30	INA	INA	INA	65.	36.	INA	INA	INA	INA	INA	Charge
2	19:53	INA	INA	INA	71.5	39.	INA	INA	INA	INA	INA	Charge
3	42:28	18.8	+4.5	1.83	57.	31.5	89	85	75	67	64	Charge
4	48:48	19.4	+4.9	1.90	62.	33.	87	84	75	67	64	Charge
5	59:30	19.9	+4.6	1.93	71.5	35.7	86	83	75	67	63	Charge
6	62:30	19.9	+4.6	1.93	73.5	37.	86	82	75	67	63	Charge
7	70:30	7.9	-4.9	0.67	75.	38.	86	82	74	67	63	Discharge

INA - Information not available as a result of oscillograph jamming caused by failure of one of the oscillographs to discharge exposed paper in the zero gravity environment. It was necessary to manually remove the paper after each run. The second unit was equipped with an automatic take-up removing the difficulty.

Table VI

FUEL CELL OPERATING PARAMETERS DURING ZERO G

FLIGHT #2

Unit	Test No.	Date	No. of Cells	No. of Cycles	No. of Cells Failed	Discharge Amps	Discharge Volts
50-W-1 (1)	1	11/15/60	10	1	1		
	2	11/22/60	10	1	1		
	3	11/23/60	10	2	1	2.0 - 10.0	8.3 - 4.3
	4	12/6/60	10	2	2	2.0 - 10.0	8.3 - 4.3
50-W-3	1	1/31/61	10	35	3	5.0 - 15.0	8.1 - 5.7
25-W-1	1	2/6/61	5	128	1	5.0 - 4.4	3.8 - 3.4
50-W-4	1	3/29/61	10	2	2	5.0 - 12.5	8.5 - 7.0
	2	4/3/61	10	1	0	—	—
	3	4/21/61	8	1	2	—	—
50-W-4A	1	5/61	10	7	0	5.0 - 8.0	7.5 - 6.5
	2	10/19/61	10	9	-	3.3 - 2.5	7.1 - 5.4
	3	10/26/61	6	19	-	2.3 - 2.0	4.8 - 3.9

(1) G. E. funded

208 cycles have been completed with multicell units on the ASD Contract.

TABLE VII

CAMERA OPERATING TIMES

FLIGHT NUMBER 2, 24 MAY 1961

Run No.	Camera On (sec.)	Camera Off (sec.)	Duration (sec.)
1	25.5	41.4	15.6
2	27.1	43.2	16.1
3	26.1	44.9	18.8
4	25.2	41.0	15.8
5	25.0	45.3	20.3
6	28.7	42.7	14.0
7	28.7	44.1	15.4
8	31.8	44.9	13.1
9	27.1	43.3	16.2
10	29.6	41.4	11.8
11	28.4	42.8	14.4
12	28.9	47.1	18.2
13	29.1	43.6	14.5
14	31.9	42.4	10.5
15	28.5	59.3	30.8
16	27.6	59.4	31.8
17	29.7	63.5	33.8
18	-2.4	74.4	76.8

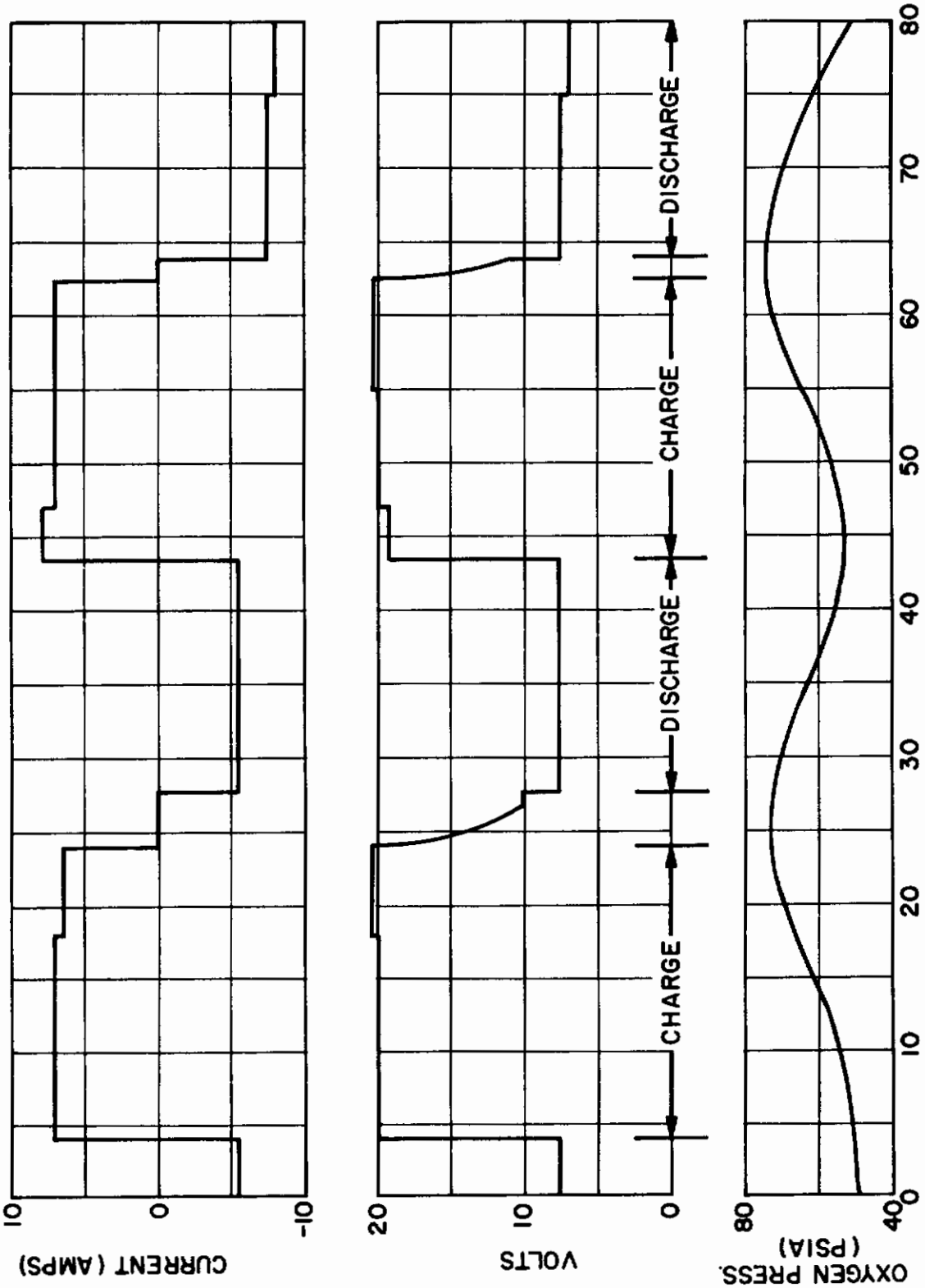

Figure 9. Time Histories of the Battery Pressure Voltage and Current During the Second KC-135 Flight

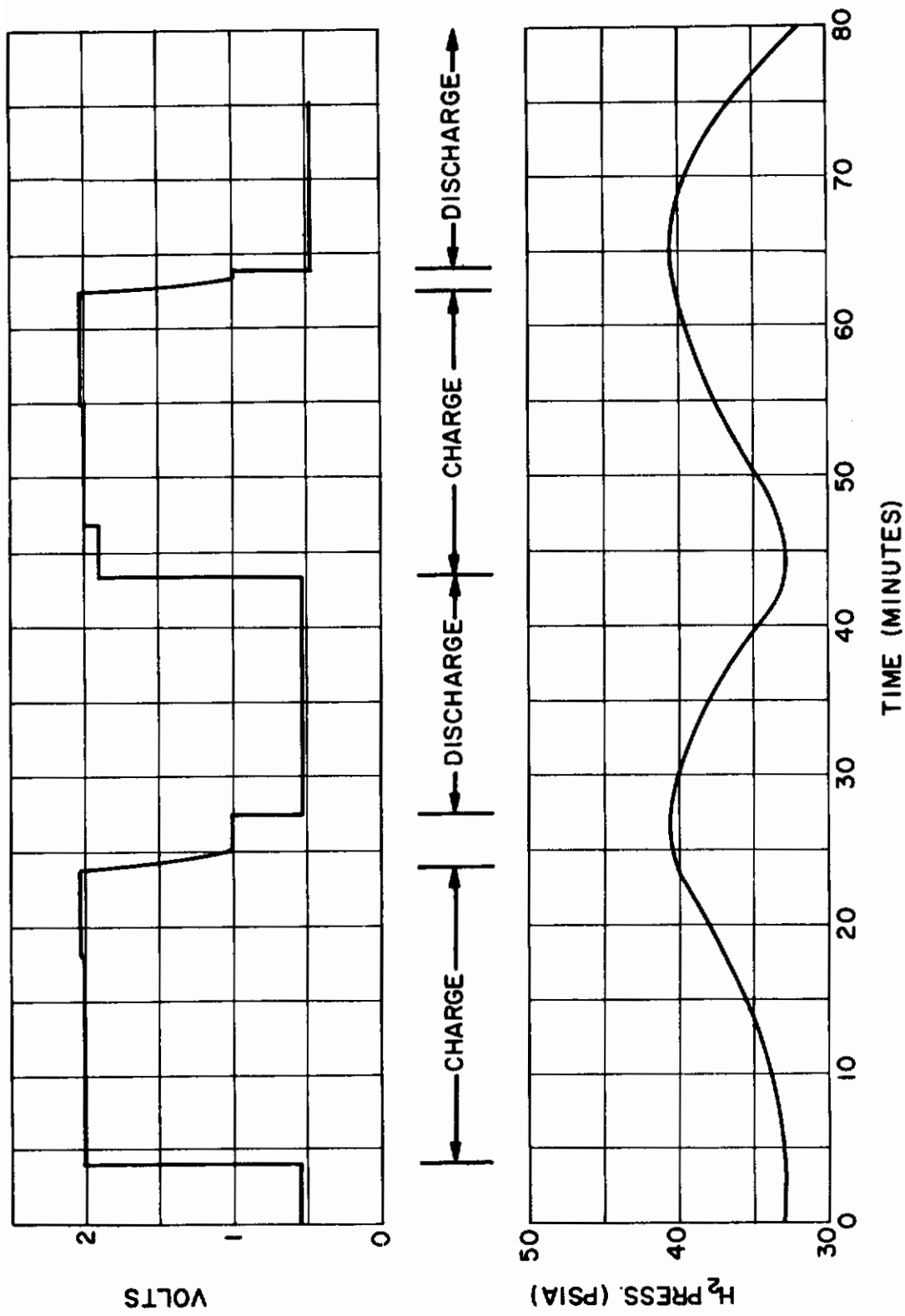

Figure 10. Time Histories of the Single Cell Pressure and Voltage During the Second KC-135 Flight

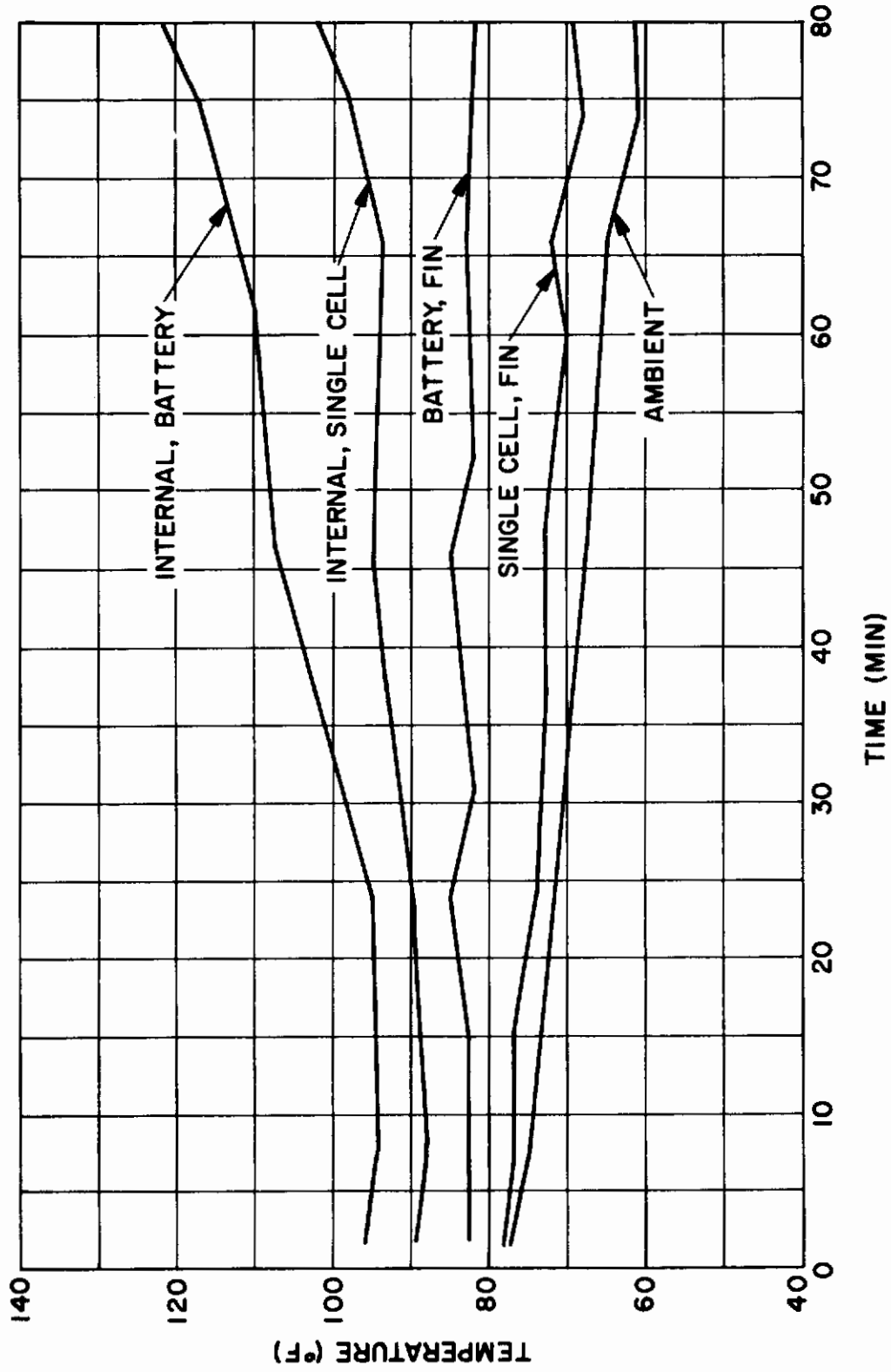

Figure 11. Time Histories of Battery and Single Cell Temperature During the Second KC-135 Flight

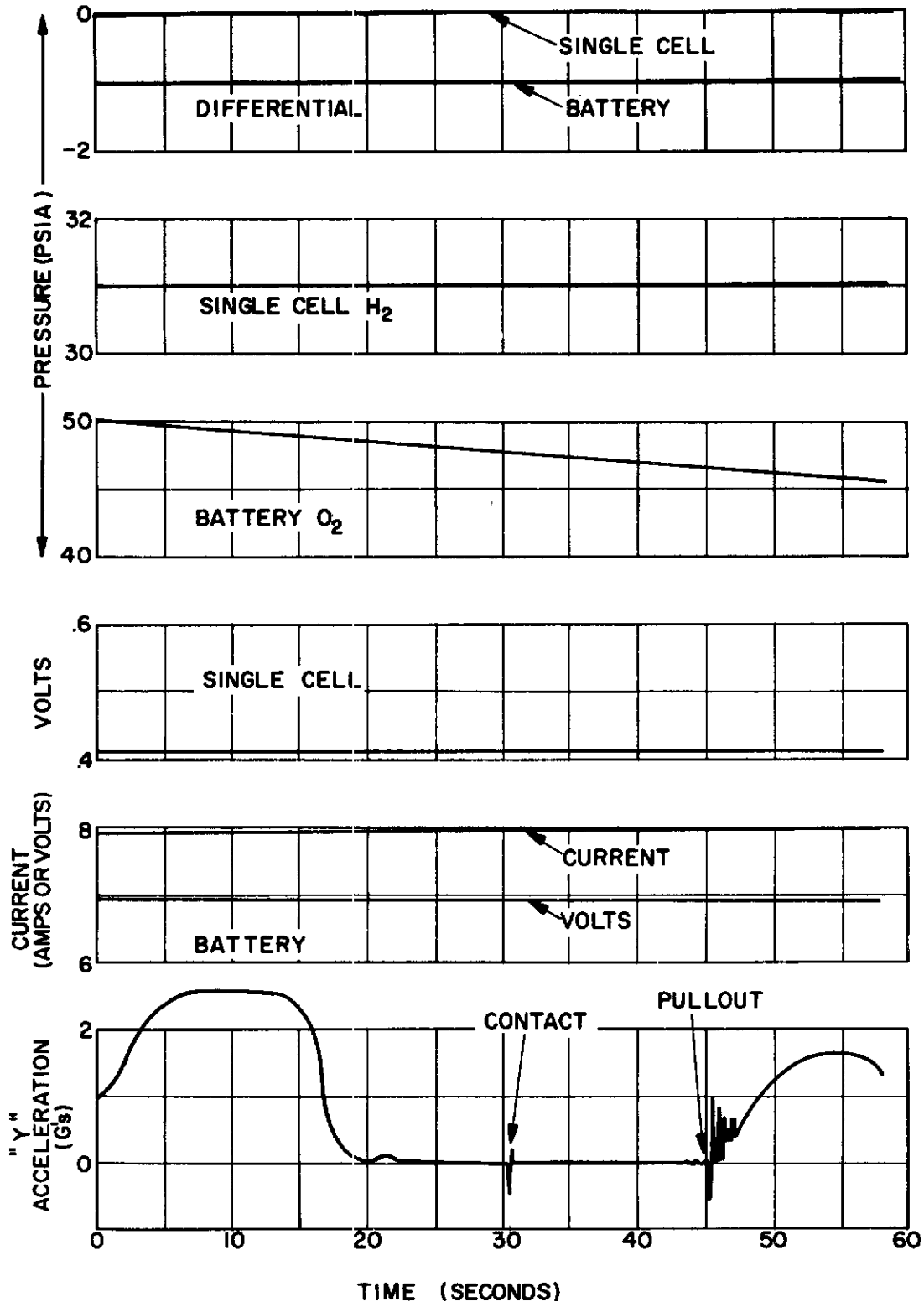

Figure 12. Time Histories of Battery and Single Cell Temperature During the Second KC-135 Flight

4.6.3 Gas Pressures

The battery was operated between the pressure limits of 55 to 75 psi during the charge-discharge cycle. The operating range of the single cell was lower (30 to 40 psia) because of the greater relative volume of the gas storage chambers used in its construction. Figure 9 shows the relationship between battery output and gas consumption and generation. The correlation between operating voltage and current drain should also be noted. The characteristic fuel cell operation parameters presented in Figure 9 are in good agreement with limited laboratory tests run on similar units.

4.6.4 Temperatures

The heat generated by a fuel cell depends on several factors: the internal resistance of the fuel cell, the activity of the electrodes, and the thermodynamics of the electrochemical reaction taking place in the cell. The 50-watt unit built for this contract was designed conservatively for heat transfer at the level of operation expected. The actual heat transfer path was from the membrane-electrode interface to the support screens and thence to the steel cell walls. Heat was radiated from the battery through the fins extending from the cell walls. As the fuel cell ages, membrane resistance increases and internal heating rises. However the conservative design was more than adequate to handle this condition.

Internal heating in the fuel cell battery was noted during the second flight as recorded by the internal thermocouples located at the membrane (Figure 11). This may be attributed to internal I^2R losses which show up as heat. The internal heating is especially evident at the higher operating rates toward the end of the second flight.

4.7 Photographic Correlation

Careful examination of all the film has shown no variation in water droplet formation due to the gravity environment encountered. There was, however, a slight change in water droplet size on going from discharge to charge. The 33 mm film, taken of the hydrogen side of the single cell, shows droplets diminishing in size from Run 2 (discharge) to Run 3 (charge). The 70 mm film taken of the oxygen size of the single cell shows droplets growing in size from Run 2 (discharge) to Run 3 (charge). Figure 13 is a 35 mm picture from Run 2 and Figure 14 is a 35 mm picture from Run 3. Figure 15 is a 70 mm from Run 2 corresponding in time to Figure 13 and Figure 16 is a 70 mm from Run 3 corresponding in time to Figure 14.

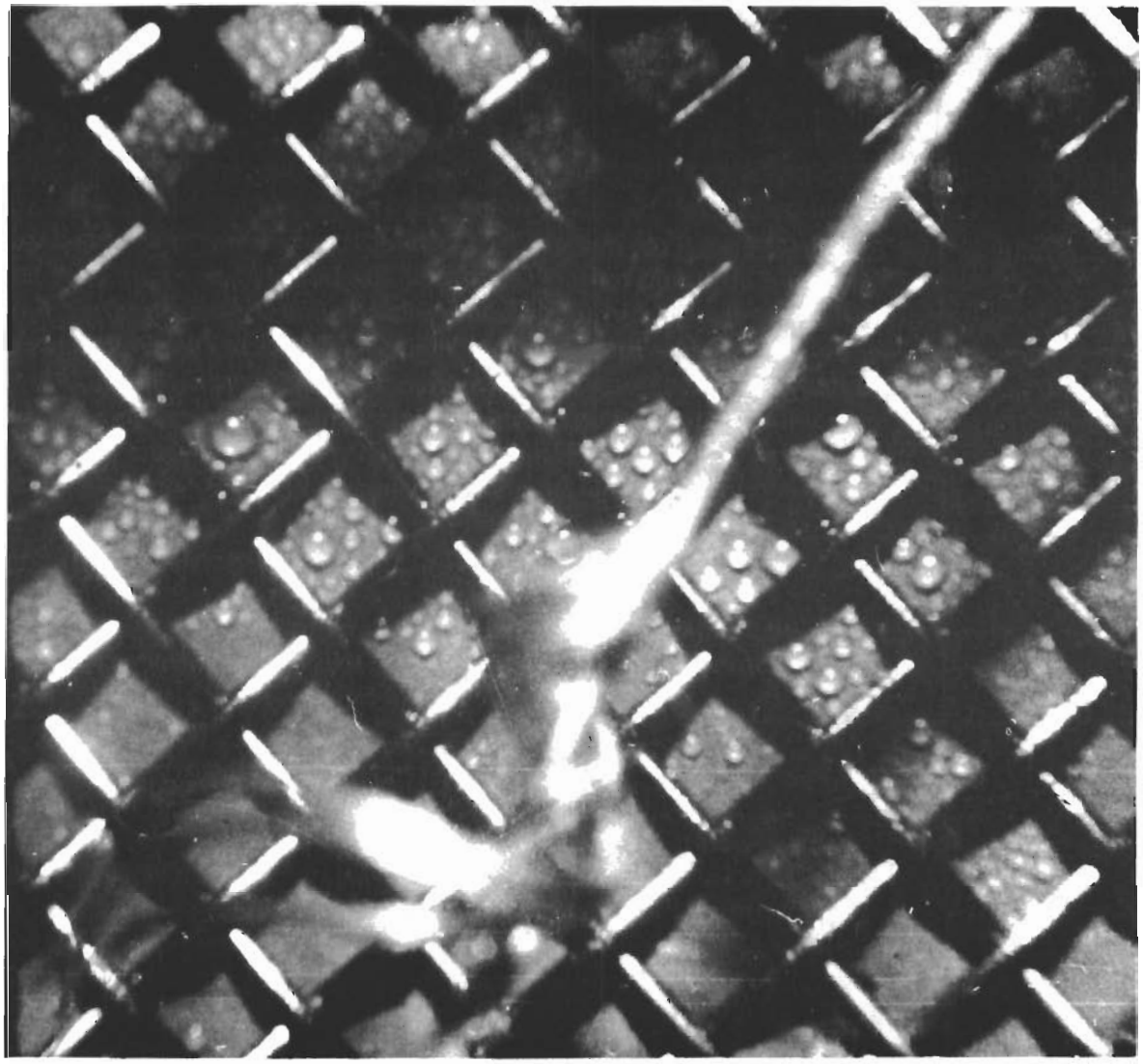

Figure 13. Single Cell, Hydrogen Side, During Discharge DC-135 0 "g" Flight - 35 mm. Camera

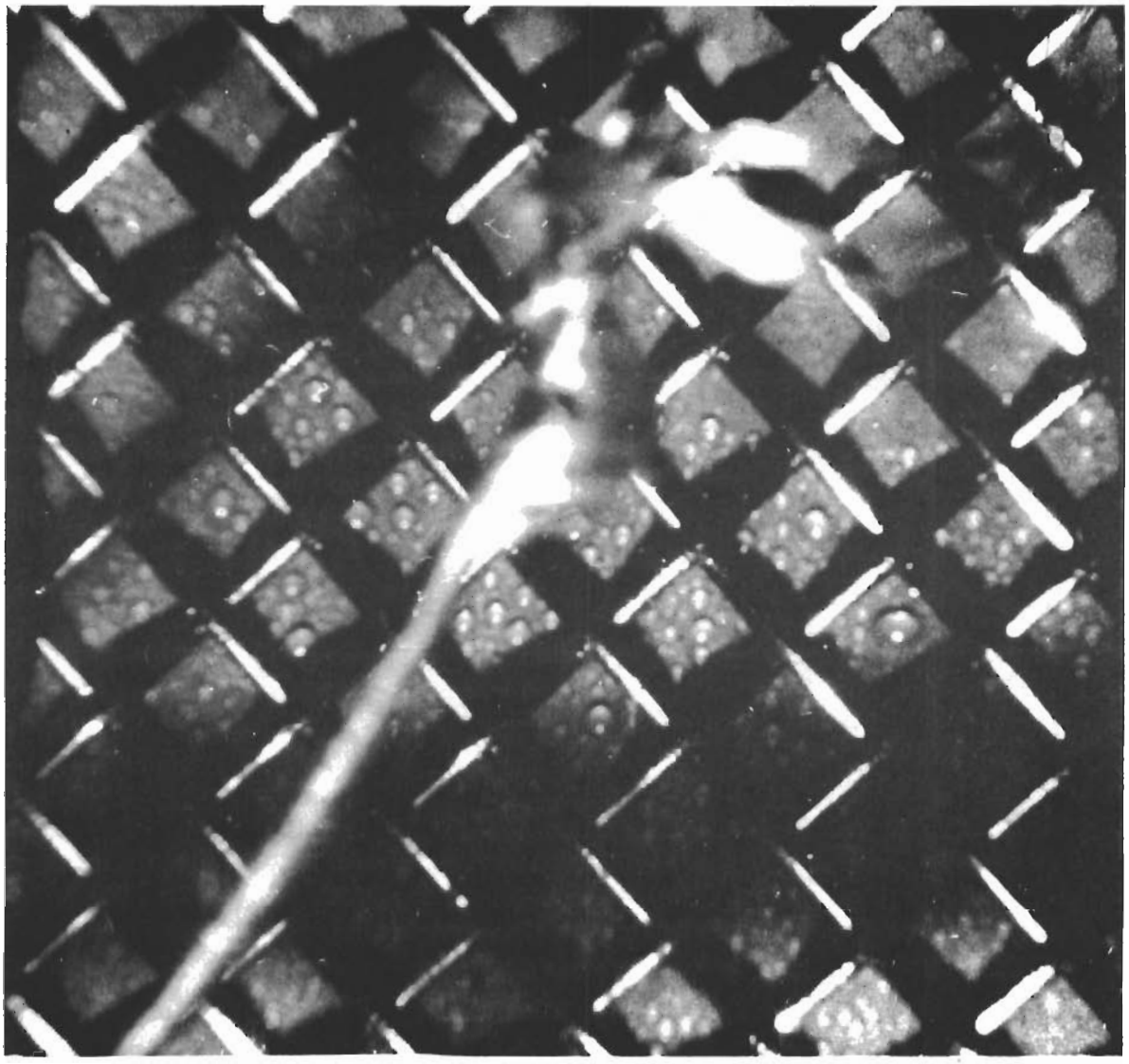

Figure 14. Single Cell, Hydrogen Side, During Charge KC-135 0 "g" Flight - 35 mm. Camera

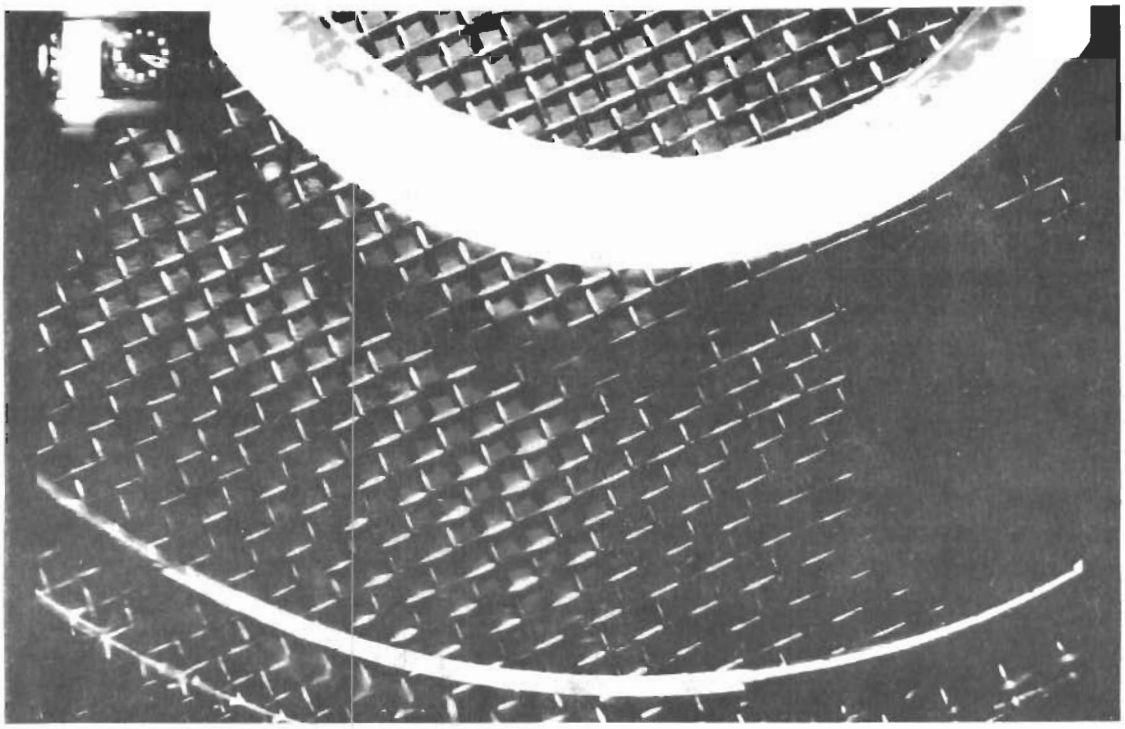

Figure 15. Single Cell, Oxygen Side During Discharge KC-135 0 "g" Flight 70 mm. Camera

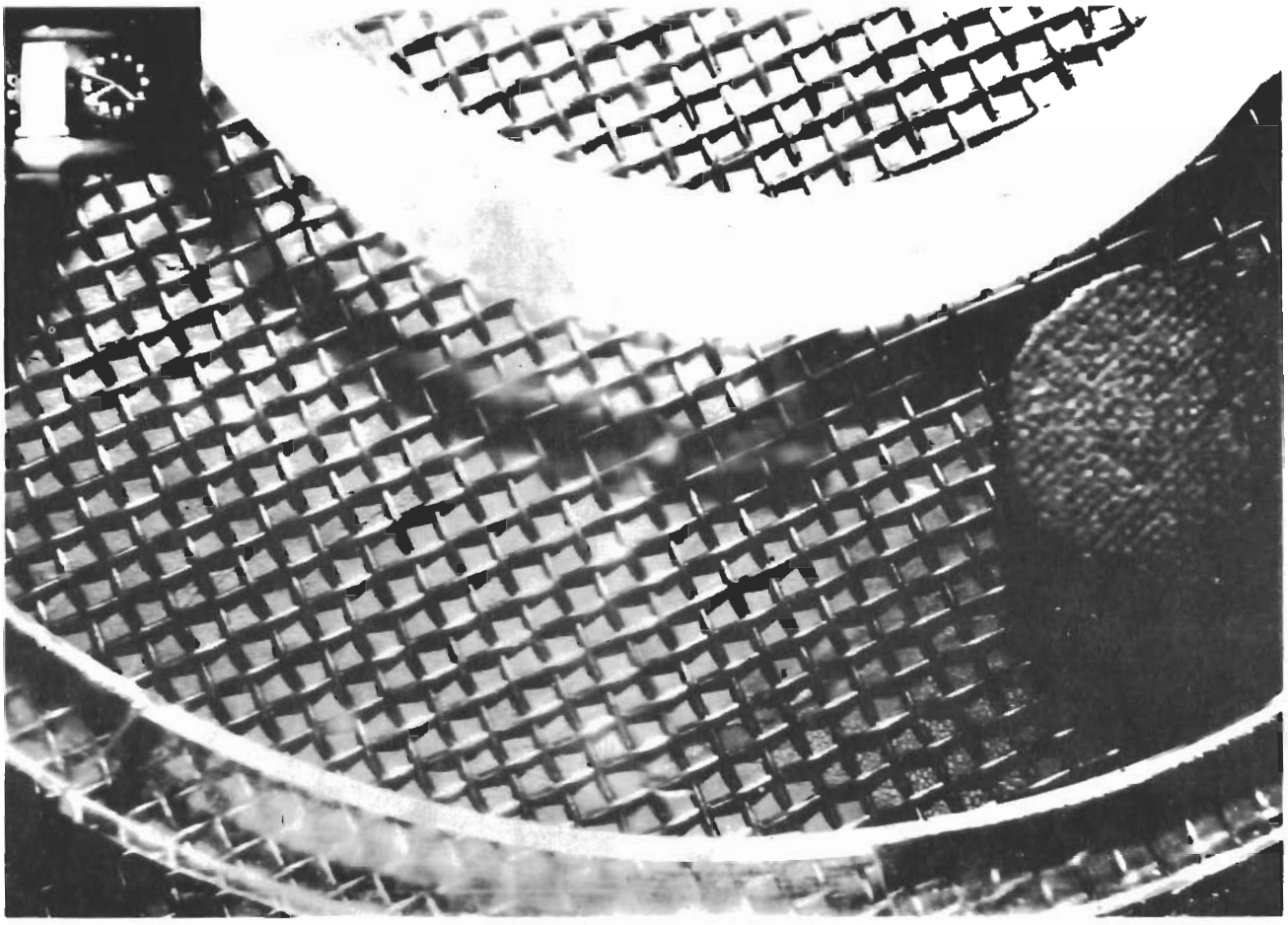

Figure 16. Single Cell, Oxygen Side During Charge KC-135 0 "g" Flight, 70 mm. Camera

The equations presented in Section 2 indicate that half the water formed on the hydrogen side during discharge is returned through the membrane and deposited on the oxygen electrode during the charge cycle. The other half of the water is electrolized into gases. Study of the photographs tend to subtantiate this. It should be noted that the water droplets do not move but change in size only.

5.0 RVX FUEL CELL MODULE

It was desired to investigate the performance of a cycling regenerative fuel cell under the conditions imposed by a 30 minute ballistic flight such as that shown in Figure 17. The method selected was to fly the fuel cell on an RVX as an experiment on a noninterference basis, meaning that the success or failure of the experiment could not effect vehicle operation. A picture of the module is shown in Figure 18 and an assembly drawing is given in Figure 19.

5.1 Test Module Description

A flight unit and a back up module were assembled. The fuel cell itself consisted of three cells with seven-inch diameter electrodes, the cell housings being 10 1/2 inches in diameter. Mounted on top of the fuel cell was a bellows chamber, and the assembly was attached to a magnesium base plate 15 1/4 inches in diameter. The overall height of the unit was six inches. This design incorporated internal manifolding of like gas spaces rather than external manifolds as used in the ten cell units. All the equipment necessary to accomplish cycling of the fuel cell during the flight was mounted on the base plate. This included a timer, relays, two pressure switches, a silver-zinc battery for in-flight charging, the required load for discharge, a pressure transducer to monitor battery pressure, and thermisters for measuring internal and external temperatures.

5.2 Operating Procedure

The timer used for the experiment was a 30-minute automatic reset type with a magnetic clutch. Upon removal of the 28 volt supply, the timer resets to zero. Several hours before lift-off the fuel cell was charged from ground power, a pressure switch cutting off the charge at 60 psig. At seal-in, a few minutes before lift-off, the fuel cell instruments were activated with vehicle power and fuel cell discharge was initiated. Four of the five telemetry channels were activated - internal and external temperature, pressure, and fuel cell voltage. At separation the timer was to have activated and continued the fuel cell discharge for an additional four minutes (total planned time of discharge was approximately ten minutes). At the start of charging, the silver-zinc battery voltage monitor was to have been activated. After ten minutes of charge, the fuel cell would have reverted back to discharge. The fuel cell was programmed to have remained on discharge until the pressure dropped to about 20 psig, at which time a pressure switch would open the circuit to prevent any of the cells from going into reverse and ruining the fuel cell.

5.3 Laboratory Tests

Laboratory tests were carried out on both modules, duplicating as closely as possible the operation and environmental conditions expected during flight.

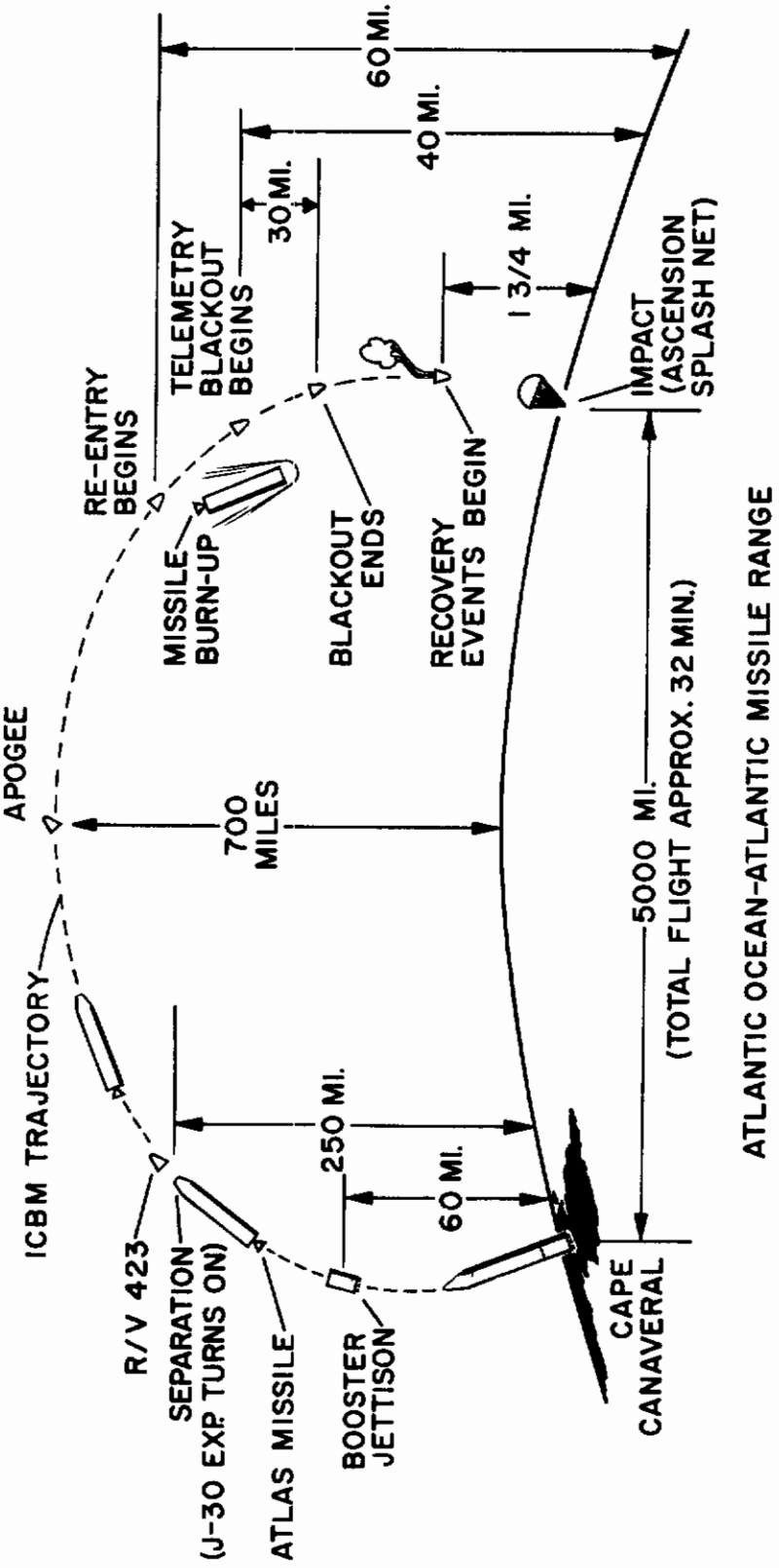

Figure 17. RVX 30 Minute Ballistic Flight Plan

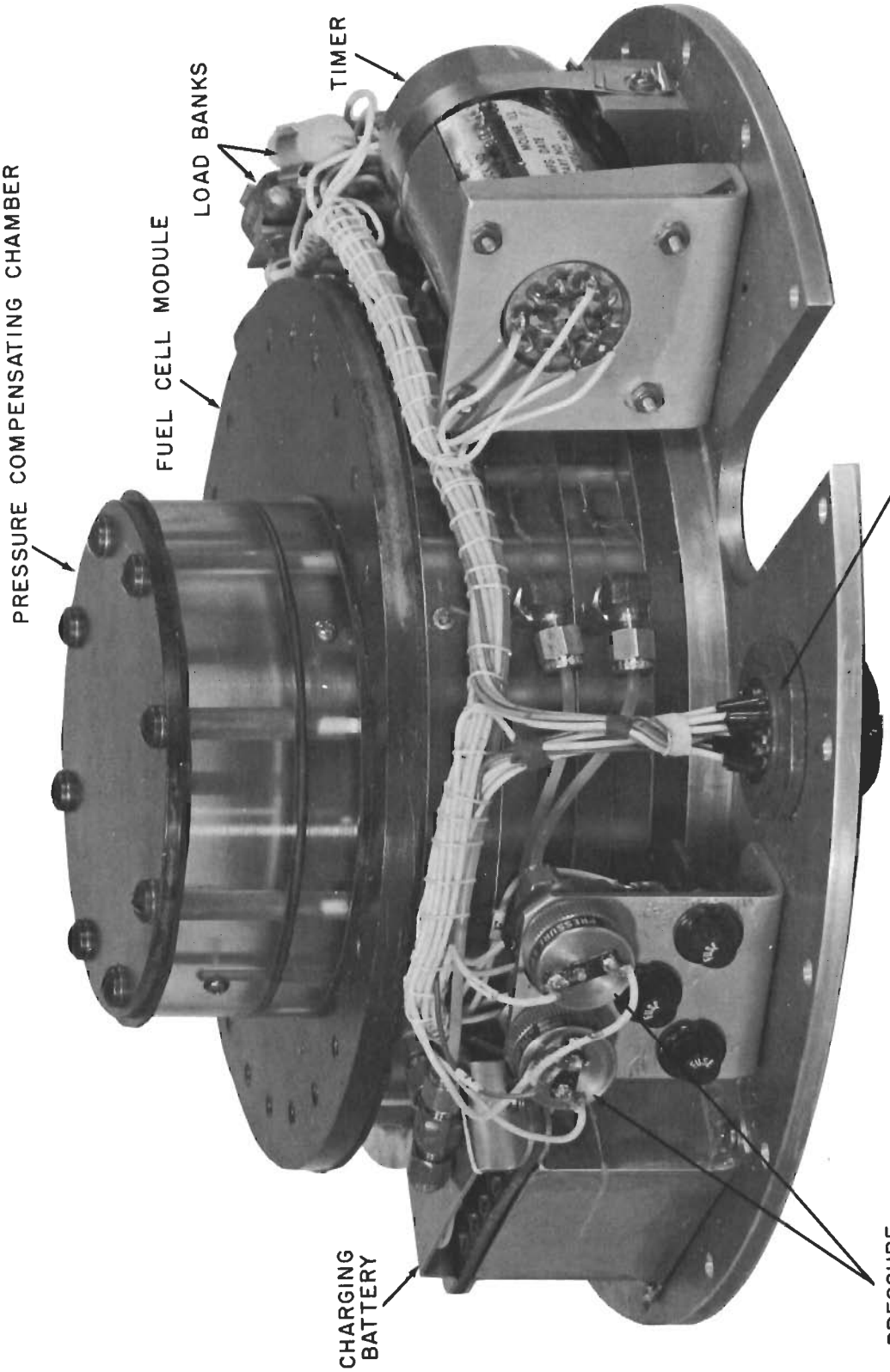

Figure 18. RVX Fuel Cell Flight Module

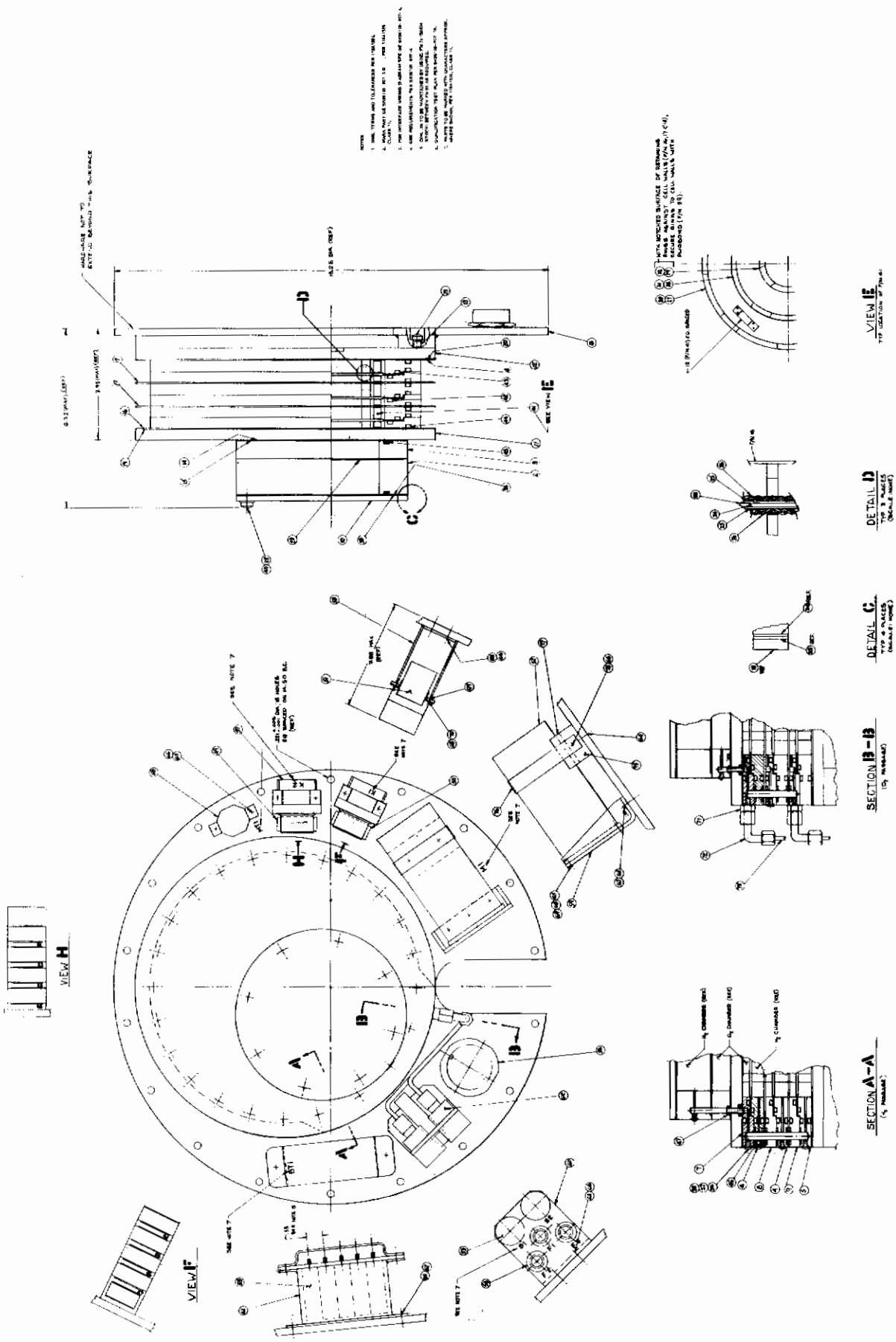

Figure 19. RVX Fuel Cell Flight Module Assembly Drawing

INDEX NUMBER	ITEM	DRAWING NUMBER
1	FUEL CELL RVX 2A	SK56105-807-5G1
2	RING, H_2 CHAMBER, BELLOWS	SK56105-807-7P1
3	RING, O_2 CHAMBER, BELLOWS	SK56105-807-8P1
4	RING, H_2	SK56105-807-9P1
5	RING, H_2	SK56105-807-9P2
6	MTG PLATE	SK56105-807-10G1
7	O_2 RING	SK56105-807-11P1
8	O_2 RING	SK56105-807-11P2
9	O_2 RING	SK56105-807-11P3
10	PLATE, BELLOWS	SK56105-807-12P1
11	END PLATE	SK56105-807-13G1
12	END PLATE	SK56105-807-13G2
13	SLEEVING	118A-1641-P18
14	INSULATION	SK56105-807-15P1
15	PLATE	SK56105-807-15P2
16	CELL WALL	SK56105-807-16P1
17	CELL WALL	SK56105-807-16P2
18	CELL WALL	SK56105-807-16P3
19	INSULATION	SK56105-807-16P4
20	INSULATION	SK56105-807-16P5
21	BOLT, 1/4 - 28 x	SK56105-807-17P1
22	BOLT, 1/4 - 28 x	SK56105-807-17P2
23	DIAPHRAGM	SK56105-807-18P1
24	MEMBRANE	SK56102-599-2P2
25	WAFER	SK56102-599-3P2
26	SCREEN	SK56102-599-4P2
27	RETAINING RING	SK56102-599-16P2
28	RETAINING RING	SK56102-599-16P3
29	RETAINING RING	SK56102-599-16P4
30	RETAINING RING	SK56102-599-16P6
31	RETAINING RING	SK56102-599-16P7
32	RETAINING RING	56102-599-16P8
33	INSULATION	56105-807-15P3
34	PLATE	56105-807-15P4
35	FILTER PAPER	
36	SCREW, FIL HD	MS-35275-26
37	LOCTITE	128A-5483
38	"O" RING	2-7-37-043
39	PLIO BOND	
40	WASHER, FLAT	AN-960-416L
41	FOIL	
42	"O" RING	2-263-37-043
43	"O" RING	2-265-37-043
44	"O" RING	2-268-37-043
45	"O" RING	2-245-37-043
46	"O" RING	2-13-37-043
47	"O" RING	2-8-37-043
48	BARORESISTOR	894-C-169-P3
49	RESISTOR	RW55V1R0
50	RESISTOR	RW55V1R2
51	RELAY 26.5 V.D.C.	FC-215
52	TIMER 28 V.D.C. -3 CIRCUITS	AR SERIES
53	PRESSURE SWITCH	C2060-6
54	FUSE HOLDER	342001
55	CELL, BATTERY	1.5 HR
56	CONNECTOR	PT-07A-22-215
57	BRACKET	SK56105-807-20G1
58	BRACKET	SK56105-807-20G2
59	SUPPORT	SK56105-807-23G1
60	BRACKET	SK56105-807-22P1
61	CHASE, BATTERY	SK56105-807-21G1
62	CONNECTOR, FEMALE	200-7-2-316
63	SCREW MACH, PAN HD	MS35216-40
64	SCREW MACH, PAN HD	MS35217-53
65	SCREW MACH, PAN HD	MS35216-26
66	WASHER, PLAIN	AN960-C8
67	WASHER, PLAIN	AN960-C10
68	WASHER, PLAIN	AN960-C6
69	NUT, SELF LOCKING	NAS-1291-C06
70	SCREW MACH PAN HD	MS35216-24
71	FITTING	SK56105-599-6P1
72	ELBOW UNION	200-9-316
73	TUBING	
74	SHIM STOCK	SK56105-807-5P1
75	BRACKET	SK56105-807-24G1
76	STRAP	SK56105-807-25P1
77	CUSHION	SK56105-807-5P2
78	SCREW MACH PAN HD	MS35216-38

5.3.1 Environmental Tests

Environmental tests for the fuel cell assembly duplicated conditions that the fuel cell would experience during launch and flight. It was decided it would be unnecessary to test the fuel cell for re-entry and impact since by this time the unit would have completed its mission. However, the hardware was shock tested to be sure the equipment would not break loose from its brackets and cause damage on impact.

Helium leak tests The fuel cell pressurized to 60 psig with helium and tested for leaks both before and after acceleration and vibration. The leak rate was determined as approximately 10^{-5} cc per minute for both tests.

Vibration The assembly was vibrated for a five-minute sweep in each of its three mutually perpendicular planes according to the following schedule:

Frequency	Amplitude
5-17.7 cps	0.49" peak to peak
17.7-1000 cps	$\pm$ 8.0 g's
1000-2000 cps	$\pm$ 4.0 g's

There was no visible damage to the fuel cell assembly.

Acceleration The assembly was subjected to an acceleration of ten g's for one minute in each of the six directions of its three mutually perpendicular axes. There was no visible damage to the fuel cell unit.

Shock The fuel cell assembly, less membranes and electrodes, was subjected to three shocks of 30 g's in a direction perpendicular to the mounting plate, the bellows chamber proceeding first in the direction of travel. The purpose of this test was to determine the safety of the fuel cell components with respect to the rest of the vehicle. If the fuel cell were to fail internally at this stage (impact), the resultant fire would be self contained and would not effect the rest of the vehicle.

No visible damage occurred to the fuel cell components as a result of this test.

5.3.2 Module Tests

Both units were operated in the laboratory to simulate the cycle expected during the RVX flight. The units were charged until the pressure switch terminated the process. Switches were activated corresponding to seal-in (T-3 minutes) and at separation. The test was terminated when the low pressure switch opened, at about 20 psig. Both units, when first assembled, performed similarly. Unit #1 was cycled both before and after the environment tests described above. No appreciable difference in performance was noted between these two tests.

Data for a typical cycle are shown in Table VIII. From these data we note that Unit #1, when originally assembled in June, delivered approximately nine watts of power on discharge. Unit #2 was assembled and tested in August.

During bench tests at AMR it was noted that both units were still functioning but at lower power levels. It was decided to rebuild Unit #1 using new membranes. Unfortunately it was necessary to use the old electrodes. When disassembled, it was observed that the internal thermister had punctured the membrane. In view of this development it was decided to rebuild the unit with two external thermisters and no internal probes. Since bench tests have shown no appreciable internal temperature change during operation of the RVX units, it was felt that this change would not markedly affect the value of the flight test results.

Unit #1 was installed in the RVX at AMR and flown.

5.4 Operation of RVX Fuel Cell #1

The fuel cell was partially charged on November 8. Following a hold on the vehicle, charging was interrupted before completion. Charging was completed November 9 at about T-5 hours. Total time required for charging was 1-3/4 hours at a rate of about 1.2 amps. Terminal fuel cell charge voltage was 6.0.

It should be noted that the fuel cell was on open circuit at full charge for over five hours without a reopening of the pressure switch. This indicates the fuel cell was well sealed and there was no leakage either internal or external.

5.5 Analysis of Data

Time histories of the measured parameters and the calculated power output of the RVX battery during launch are given in Figures 20 and 21.

Silver-zinc battery voltage was not programmed to record before the fuel cell would have gone into charge at four minutes after separation. The temperature thermistors reported reliable and consistent information indicating an external temperature of 21 degrees C. A gradual drop off in pressure with discharge was noted as expected. From seal-in at T-212.5 seconds the fuel cell voltage shows a rather sharp drop in performance, stabilizing at about 1.0 volts. This performance is attributed to old electrodes used in the reassembled unit. The voltage stabilized and indeed started to improve as expected after about six minutes of discharge. (Figure 20)

From bench tests on Unit #1 it was observed that the actual voltage measured between the positive and negative terminals of the fuel cell was higher than that read through telemetry. An analysis of the data and the circuit revealed that

TABLE VIII

RVX FUEL CELL MODULE TEST, UNIT #1

Time	Function	Fuel Cell		Temp. °F		Press.	Chg. Battery
		Volts	Amps (1)	Int.	Ext.	PSIG	Volts (2)
2	GSE Chg.	5.4	6.0				9.2
8		5.6	6.0				
20		6.1	6.0				
26		6.0	4.5				
34		6.1	4.2				
35	Off						
T-3	Seal-in						
-2	Disch.	2.15	4.3	82	84	59	
0	Disch.	2.10	4.2				
+1	Sep.						
+2	Disch.	2.10	4.2	86			
+5	Chg.	5.2	3.9		90	48	7.2
+10	Chg.	5.4	3.0		90	54	6.9
+13	Chg.					58	
+17	Disch.	2.2	4.4	84	88	54	
+30	Disch.	2.15	4.3	82	90	36	
+40	Disch.	2.0	4.0			23	
+42	O.C.					20	

(1) Amps calculated using $R_{ch.}$ and $R_{disch.}$ = 0.5 ohms

$$I_{ch.} = \frac{(E_{Ag-Zn}) - (E_{F.C.})}{R_{ch.}}$$

$$I_{disch.} = \frac{E_{F.C.}}{R_{disch.}}$$

E_{Ag-Zn} is voltage of charge battery

(2) Charge battery monitor programmed to record only during fuel cell charge

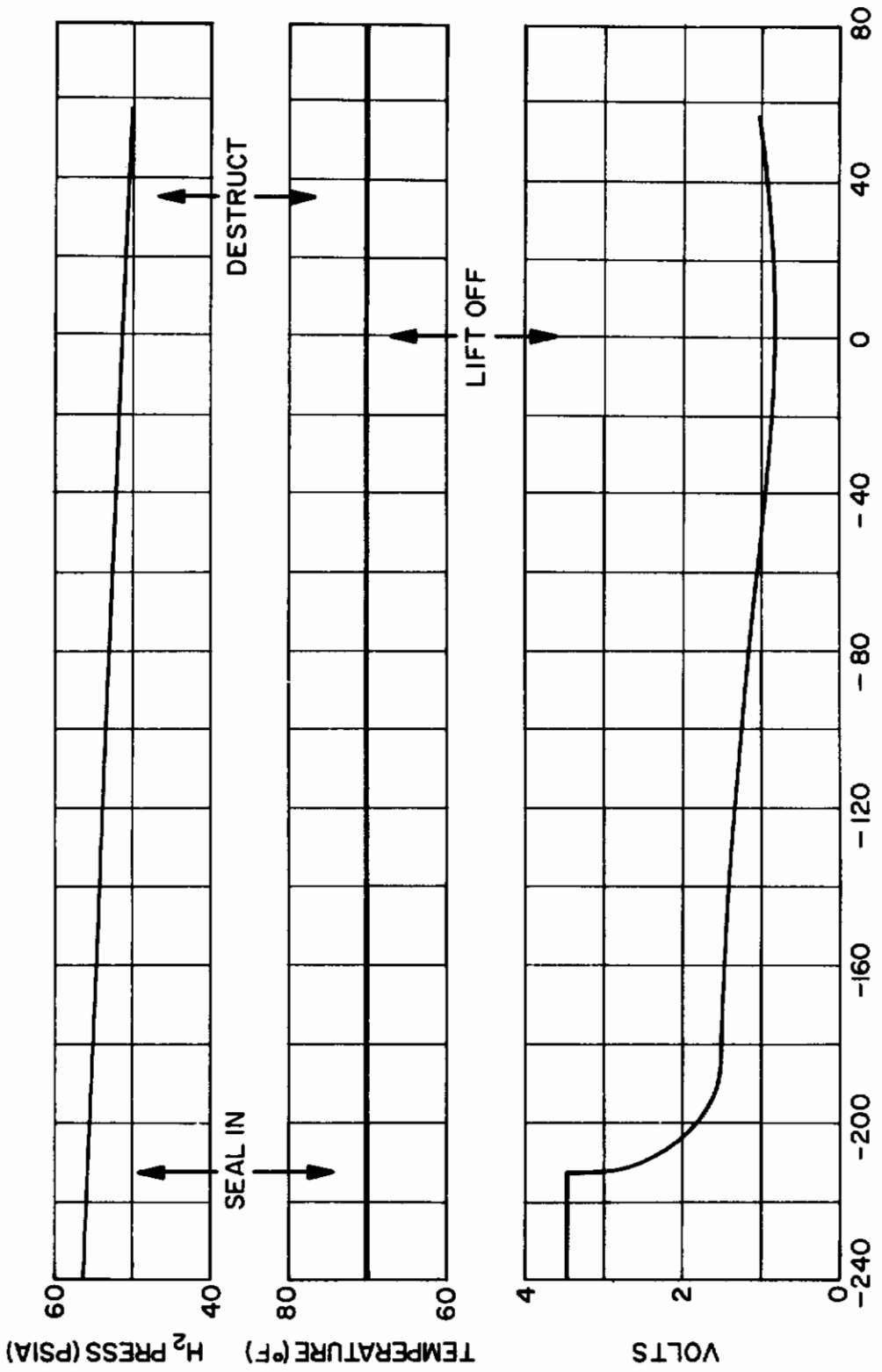

Figure 20. Time Histories of Voltage Temperature and Pressure of the RVX Flight Unit During Launch

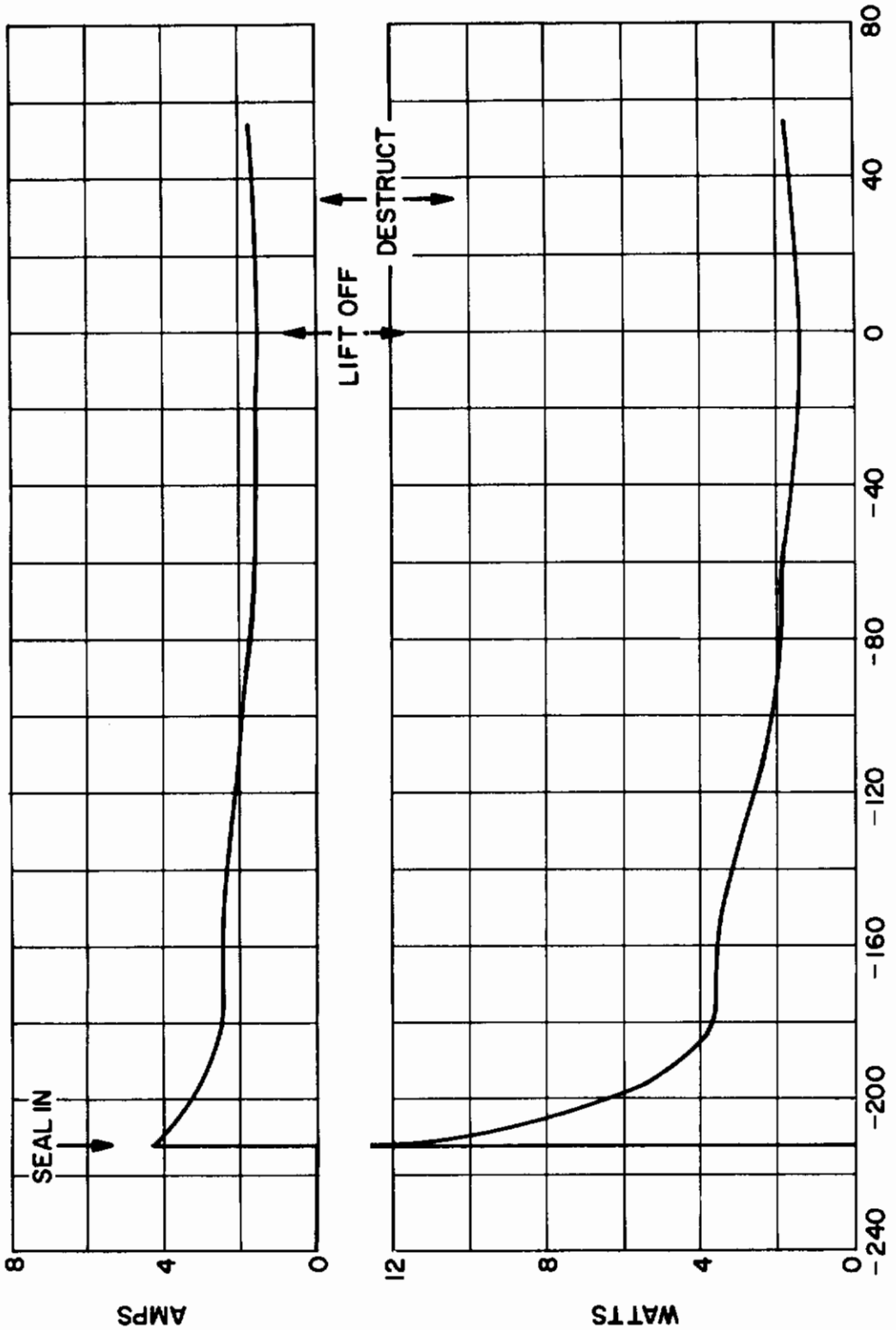

Figure 21. Time Histories of Measured Current and Calculated Power of the RVX Flight Unit During Launch

this voltage difference was caused by additional resistance in the discharge circuit. The true discharge circuit resistance was calculated to be 0.6 ohm. Actual as opposed to measured fuel cell voltage is plotted in Figure 20.

5.6 Unit #2

The unit built as a back-up for the RVX was delivered to ASD for further cycle testing.

6.0 CONCLUSIONS

Cycling tests carried out utilizing a 90-minute charge-discharge cycle have shown single fuel cells to be capable of continued operation for periods of six months. Continuous design improvements on the multicell units resulted in progressively better performance, however, operation of the multicell units was not as satisfactory as single cells. Uneven electrode support in the multicell units is believed to cause high internal resistance and consequently limited life.

An analysis of data obtained from operating fuel cells during limited-time zero gravity runs aboard an aircraft have shown no appreciable effect on fuel cell operation as a result of the environments encountered. Periods of weightlessness varied between ten and 20 seconds and g loading varied between zero and 2 1/2.

An attempt to obtain data on a cycling fuel cell during a 30 minute ballistic flight aboard an RVX was minimized when the vehicle had to be destroyed shortly after life-off. However, data was obtained for about 35 seconds of flight which indicated the fuel cell to be operating satisfactorily.

7.0 RECOMMENDATIONS

Several promising electrode fabrication techniques have been uncovered. These techniques circumvent the electrode membrane electrical contact problem which is believed to be the only reason multicell cycle life has not realized the up to six months cycle-life single cells have already achieved. The Missile and Space Vehicle Department strongly recommends that a program consisting of fabrication of two exploratory single cells and two multicell batteries incorporating the new fabrication techniques be persued. One of the multicell units would be flown "piggy back" on another space lab experimental flight to obtain the urgently needed 30-minute zero g performance during actual cycling conditions of the anionic membrane process that was lost on the present program because of the RVX vehicle failure during powered flight. The other multicell unit should be subjected to life cycle testing to establish the expected long cycle-life of the redesigned unit.